Oxford Research Encyclopedia of Climate Science

Predictability of El Niño-Southern Oscillation Events

Wansuo Duan and Mu Mu

Subject: Climate Systems and Climate Dynamics Online Publication Date: Mar 2018
DOI: 10.1093/acrefore/9780190228620.013.80

Summary and Keywords

This article retrospects the studies of the predictability of El Niño-Southern Oscillation (ENSO) events within the framework of error growth dynamics and reviews the results of previous studies. It mainly covers (a) the advances in methods for studying ENSO predictability, especially those of optimal methods associated with initial errors and model errors; and (b) the applications of these optimal methods in the studies of "spring predictability barrier" (SPB), optimal precursors for ENSO events (or the source of ENSO predictability) and target observations for ENSO predictions. In this context, some of major frontiers and challenges remaining in ENSO predictability are addressed.

Keywords: El Nino, predictability, initial errors, model errors, nonlinearity, optimal perturbations

Introduction

The El Niño-Southern Oscillation (ENSO) is characterized by the interannual variability in sea surface temperatures (SSTs) in the tropical Pacific (Kao & Yu, 2009; Philander, 1983; Ropelewski & Halpert, 1987; Wang & Picaut, 2004; Weng, Ashok, Behera, Rao, & Yamagata, 2007). Although the ENSO phenomenon originates and develops in the tropical Pacific, it has global climatic, ecological, economic, and social impacts through oceanic and atmospheric teleconnections (Alexander et al., 2002; Bjerknes, 1969; Cane, 1983; Ham, Sung, An, Schubert, & Kug, 2014; Hoerling, Kumar, & Zhong, 1997; McPhaden, Zebiak, & Glantz, 2006; Rasmusson & Wallace, 1983; Trenberth et al., 1998). ENSO forecasts are therefore important for reducing the resulting natural disasters and supplying valuable information for agriculture, fisheries, forestry, and many other climate-sensitive human endeavors.

Significant progress has been made in ENSO theory and predictions over the years, especially through the TOGA (Tropical Ocean Global Atmosphere) program (see the review by Wang & Picaut, 2004). These endeavors have deepened the understanding of

ENSO dynamics and improved the accuracy of ENSO predictions. The ENSO is skillfully predictable with one- to two-year lead times in hindcast experiments (Chen, Cane, Kaplan, Zebiak, & Huang, 2004; Fedorov & Philander, 2000; Kirtman & Schopf, 1998; Luo, Masson, Behera, & Yamagata, 2008). However, there are still considerable uncertainties in real-time ENSO predictions (Duan & Wei, 2012; Jin et al., 2008; Tang, Kleeman, & Moore, 2008), and the practical prediction skill is presently limited to six months (Kirtman et al., 2002; Mu & Ren, 2017). Especially after the 1990s, a new type of El Niño event, often called central Pacific–El Niño (CP-El Niño) events have occurred frequently and increased the uncertainties of ENSO predictions. Hendon, Lim, Wang, Alves, and Hudson (2009) had limited success in predicting the differences between the two El Niño types using the Australian Bureau of Meteorology's Predictive Ocean Atmosphere Model for Australia (POAMA) coupled seasonal forecast model, and the effective prediction skill was achieved only one month ahead. Even when an ensemble forecast technique was used to predict the two types of El Niño events, useful prediction skill was only possible with a four-month lead time (Jeong et al., 2012).

The so-called CP-El Niño events have also been variously termed "dateline El Niño" (Larkin & Harrison, 2005), "El Niño Modoki" (Ashok, Behera, Rao, Weng, & Yamagata, 2007; Takahashi, Montecinos, Goubanova, & Dewitte, 2011), and "warm pool El Niño" (Kug, Jin, & An, 2009). The CP-El Niño events are different from traditional El Niño events—that is, eastern Pacific–El Niño (EP–El Niño) events (Rasmusson & Carpenter, 1982). The former type has warm SSTs concentrated in the central Pacific (Ashok et al., 2007; Kao & Yu, 2009; Kug et al., 2009); whereas the latter has warm SSTs centered in the eastern Pacific. Furthermore, the CP-El Niño events significantly influence temperature and precipitation over many parts of the globe but in a manner different from that of traditional EP-El Niño events (see, e.g., Weng et al., 2007). Although interest in the two types of El Niño events has recently increased, simulating and predicting the CP-El Niño, in contrast to the EP-El Niño, remains a challenge.

Predictability studies could provide useful information on reducing the prediction uncertainties for the two types of ENSO events. The so-called predictability is a fundamental issue in both atmospheric and oceanic research, as well as in numerical weather and climate prediction. It indicates the extent to which even minor imperfections in the knowledge of the current state or the representation of the system limit knowledge of subsequent states (Kirtman et al., 2013). Studies of predictability have received considerable attention in recent decades thanks to the pioneering work of the atmospheric scientist Lorenz in the early 1960s (Lorenz, 1962A, 1962B, 1963, 1965, 1969). One of the great efforts is the exploration of the fundamental limits to predictability (Smith, Ziehmann, & Fraedrich, 1999). The predictability of a system is strongly dependent on its stability properties (Moore & Kleeman, 1996; Smith et al., 1999). If the system is particularly unstable, any initial uncertainty that projects significantly onto one of these instabilities will severely limit the skill of an initial-value forecast. Lorenz (1975) showed that the extreme sensitivity of weather predictions to initial conditions means that detailed forecasts are, in general, impossible beyond approximately two weeks. This kind of initial-value problem is referred to as the first kind of predictability problem (Lorenz, 1975). In studies of the first kind of predictability problem, the models are usually assumed to be perfect. The second kind of predictability problem aims to estimate how a given dynamic system responds to a change in some prescribed parameter or external forcing (Lorenz, 1975). The response of the ENSO to stochastic forcing related to the Madden-Julian Oscillation (MJO), westerly burst events, and the like, or the response of an atmospheric general circulation model (GCM) to a prescribed change in SSTs, are problems related to the second kind of predictability (Moore & Kleeman, 1999; Torn, 2016; Zebiak, 1989). Uncertainties in such predictions may arise from the accuracy in the prescribed change itself, or from uncertainties in model formulation. In practice, many forecasts do not fall exclusively into either of these two categories. Therefore, estimating prediction uncertainties caused by initial errors or model errors, or both, are of central importance in studies of predictability problems. Tennekes (1991) argued that no forecast was complete without an estimate of the prediction error. This perspective can be traced back to Thompson (1957). Since then, operational weather forecasting has progressed to the point of explicitly attempting to quantify the evolution of the initial uncertainty during each forecast (Palmer, Branković, Viterbo, & Miller, 1992; Toth & Kalnay, 1996), which, furthermore, has been propagated through coupled model forecasts during recent decades, even in climate decadal predictions (Ding, Keenlyside, Latif, Park, & Wahl, 2015; Hawkins & Sutton, 2009; Wu & Zhou, 2012).

For the coupled ocean-atmosphere phenomenon represented by ENSO events, quite a few studies have investigated their related predictability problems and have especially explored them from the perspective of error growth dynamics with the purposes of identifying the sources of prediction errors and exploring methods to reduce prediction error. These two purposes are right the ones of “predictability studies” summarized by Mu, Duan, and Chou (2004). Great achievements have been obtained and useful ideas have been proposed for improving ENSO forecast skill.

Advances in Methods for Estimating ENSO Predictability

Despite the consensus on the best approach for predicting large dynamical systems such as the Earth’s atmosphere, optimal methods for quantifying the predictability remain the subject of debate. One of the approaches based on optimal growth is the linear singular vector (LSV) method, which was first introduced to meteorology by Lorenz (1965) and is established on the basis that the evolution of initial perturbations can be described approximately by the tangent linear model (TLM). However, due to its lack of nonlinearity, the LSV method has difficulty describing the nonlinear optimal growth of the finite amplitude of initial perturbations and then fails to reveal the initial errors that cause the largest prediction errors in predictability studies of atmospheric and oceanic flows. For model errors, Kleeman and Moore (1997) developed an approach, called the (linear) stochastic optimal approach, to study problems in ENSO predictability caused by model errors. Barkmeijer, Iversen, and Palmer (2003), however, did not think that the stochastic optimal approach was feasible in a realistic high-dimensional numerical model because of the explicit matrix computation of the linear model propagator and its adjoint. To compensate for this limitation, Barkmeijer et al. (2003) proposed an approach using (linear) forcing singular vectors (FSVs), which are constant in time but represent the tendency perturbations that lead to significant perturbation growth in a linearized model during a given forecast period. The FSV method is derived using a linear approximation to a nonlinear model (the linearized model), which raises concerns about the validity of the linearized model and the effects of nonlinear physical processes and whether limitations exist due to its linearization.

Optimal Initial Perturbation: From Linear Singular Vector to Conditional Nonlinear Optimal Perturbation

An evolution equation for the state vector $\boldsymbol{U}$ can be written as follows, where $\boldsymbol{U}$ may represent surface current, thermocline depth, and sea surface temperature, and so on.

$$\begin{cases} \frac{\partial U}{\partial t} = F(U(x,t)), \\ U\big|_{t=0} = U_0, \end{cases} \quad \text{in } \Omega \times [0,\tau] \qquad (1)$$

where $\boldsymbol{U}(\boldsymbol{x},t) = (\boldsymbol{U}_1(\boldsymbol{x},t), \boldsymbol{U}_2(\boldsymbol{x},t), \cdots, \boldsymbol{U}_n(\boldsymbol{x},t))$; $\boldsymbol{U}_0$ is the initial state; $(\boldsymbol{x},t) \in \Omega \times [0,\tau]$, in which Ω is a domain in R^n, $\boldsymbol{x} = (x_1, x_2, \cdots, x_n)$ and t is time; and $\tau < +\infty$ is the final time of the evolution of state variables. F is a nonlinear operator. Assuming that the Eq. (1) and the initial state are known exactly, the future state can be determined by integrating Eq. (1).

Let $\boldsymbol{M}_t$ be a propagator (i.e., numerical model) of the Eq. (1), which propagates the initial value to the future time t. $\boldsymbol{u}_0$ is an initial perturbation superposed on a basic state $\boldsymbol{U}(\boldsymbol{x},t)$, which is a numerical solution to the nonlinear model and satisfies $\boldsymbol{U}(\boldsymbol{x},t) = \boldsymbol{M}_t(\boldsymbol{U}_0)$ ($\boldsymbol{U}_0$ is the initial value of $\boldsymbol{U}(\boldsymbol{x},t)$). Then

$$\boldsymbol{M}_t(\boldsymbol{U}_0 + \boldsymbol{u}_0) = \boldsymbol{U}(\boldsymbol{x},t) + \boldsymbol{u}(\boldsymbol{x},t), \quad (2)$$

so $\boldsymbol{u}(\boldsymbol{x},t)$ describes the evolution of the initial perturbation $\boldsymbol{u}_0$.

Linear Singular Vector

The LSV is derived from a linearized model of the Eq. (1) and represents the fastest-growing initial perturbation superimposed on the basic state $\boldsymbol{U}(\boldsymbol{x},t)$. Let $\boldsymbol{L}_t$ be the linearized counterpart of nonlinear propagator $\boldsymbol{M}_t$. The LSV is then obtained by solving

$$\lambda(\boldsymbol{u}_0^l) = \max_{\boldsymbol{u}_0} \frac{\|\boldsymbol{L}_t(\boldsymbol{u}_0)\|}{\|\boldsymbol{u}_0\|}, \quad (3)$$

where $\boldsymbol{u}_0^l$ is the LSV and λ is the linear singular value (i.e., the growth rate of the LSV). For any constant c, the vector $c\boldsymbol{u}_0^*$ is also an LSV. Furthermore, for different c, the LSVs $c\boldsymbol{u}_0^*$ correspond to the same linear singular value.

The LSV represents the fastest-growing initial perturbation in linearized models and attempts to represent the initial error that has the largest effect on prediction uncertainties. The LSV method has been widely used to address problems related to error growth in the predictability of ENSO (Moore & Kleeman, 1996; Moore et al., 2006; Xue, Cane, & Zebiak, 1997A; also see the section "Conditional Nonlinear Optimal Perturbation") and other weather and climate events (Palmer, Buizza, Molteni, & Corti, 1994; Palmer & Zanna, 2013; Tziperman & Ioannou, 2002; Yamaguchi, Iriguchi, & Nakazawa, & Wu, 2009; Zanna, 2012). Especially, the LSVs have been adopted by the ECWMF (European Centre for Medium-Range Weather Forecasts) to conduct the ensemble forecasts for weather and have made great achievements (Palmer & Zanna, 2013).

Conditional Nonlinear Optimal Perturbation

To study the effect of nonlinearity on the fastest growing initial perturbation, Mu, Duan, and Wang (2003) proposed a novel approach of the conditional nonlinear optimal perturbation (CNOP). The CNOP describes the initial perturbation that has the largest nonlinear evolution at prediction time. For a chosen norm $\|\cdot\|$, an initial perturbation $\boldsymbol{u}_{0\delta}$ is termed the CNOP if and only if

$$J\left(\boldsymbol{u}_{0\delta}^{n}\right)=\max_{\|\boldsymbol{u}_0\|\leq\delta}J\left(\boldsymbol{u}_0\right),\ (4)$$

where

$$J\left(\boldsymbol{u}_0\right)=\|\boldsymbol{M}_t\left(\boldsymbol{U}_0+\boldsymbol{u}_0\right)-\boldsymbol{M}_t\left(\boldsymbol{U}_0\right)\|,\ (5)$$

$\|\boldsymbol{u}_0\|\leq\delta$ is the constraint condition of the initial perturbation amplitudes defined by the chosen norm $\|\cdot\|$, where the constraint condition is simply expressed as belonging to a ball with the chosen norm. The norm $\|\cdot\|$ also measures the evolution of the perturbations. Of course, one can also choose other metrics to evaluate the amplitudes of initial perturbations and their growth, as appropriate for particular physical problems. Mathematically, the CNOP is the global maximum of $J\left(\boldsymbol{u}_0\right)$ over the ball $\|\boldsymbol{u}_0\|\leq\delta$. It is also possible that there exist local maximum values of $J\left(\boldsymbol{u}_0\right)$; in such cases, the corresponding maximum is a local CNOP.

The CNOP is defined by directly using a nonlinear model and an extension of LSV in a nonlinear field. When the bound of initial constraints is very small, the LSV can approximate the CNOP; when the initial perturbations are large, the LSV's approximation to the CNOP does not hold (Duan, Mu, & Wang, 2004; Mu & Zhang, 2006). In this case, the CNOP represents the perturbations that have the largest nonlinear evolution at prediction time. The CNOP method is superior to the LSV method in identifying nonlinear effects (Duan & Mu, 2009).

Existing numerical models are unable to describe atmospheric and oceanic motions exactly, and contain model errors. Uncertainties in model parameters represent an important source of model errors (Lu & Hsieh 1998; Mu, Duan, & Wang, 2002). Mu, Duan, Wang, and Zhang (2010) extended the CNOP approach just described to explore the predictability limit related to the error modes of the model parameters and renewed the CNOP, including not only the optimal initial perturbation but also the optimal model parameter perturbation. If one writes the Eq. (1) as follows:

$$\begin{cases} \frac{\partial \boldsymbol{U}}{\partial t} + \boldsymbol{F}(\boldsymbol{U}, \boldsymbol{P}, t) = 0 \\ \boldsymbol{U}|_{t=0} = \boldsymbol{U}_0 \end{cases}, \quad (6)$$

where $\boldsymbol{P} = (p_1, p_2, \cdots, p_m)$ is the model parameter vector and other variables are as in Eq. (1). Assuming perfect initial conditions and uncertainties in model parameter $\boldsymbol{P}$, then the corresponding Eq. (2) becomes

$$\boldsymbol{U}(\tau) = \boldsymbol{M}_t(\boldsymbol{P})(\boldsymbol{U}_0), \ \boldsymbol{U}(\tau) + \boldsymbol{u}_p(\tau) = \boldsymbol{M}_t(\boldsymbol{P} + \boldsymbol{p}')(\boldsymbol{U}_0), \quad (7)$$

where $\boldsymbol{u}_p(t)$ describes the departure from the basic state $\boldsymbol{U}(t)$ caused by parametric error $\boldsymbol{p}'$.

Considering the existence of both an initial perturbation and parametric perturbation in Eq. (2), it has

$$\boldsymbol{U}(\tau) = \boldsymbol{M}_t(\boldsymbol{P})(\boldsymbol{U}_0), \ \boldsymbol{U}(\tau) + \boldsymbol{u}_{I,p}(\tau) = \boldsymbol{M}_t(\boldsymbol{P} + \boldsymbol{p}')(\boldsymbol{U}_0 + \boldsymbol{u}_0), \quad (8)$$

where $\boldsymbol{u}_{I,p}(t)$ is the departure from the basic state $\boldsymbol{U}(t)$ caused by the combined mode of the initial and model parameter perturbations.

The nonlinear optimization problem is defined as follows:

$$J_1(\boldsymbol{u}_{0\delta}, \boldsymbol{p}'_\sigma) = \max_{\boldsymbol{u}_0 \in C_\delta, \boldsymbol{p}' \in C_\sigma} J(\boldsymbol{u}_0, \boldsymbol{p}'), \quad (9)$$

where

$$J(\boldsymbol{u}_0, \boldsymbol{p}') = \| \boldsymbol{M}_t(\boldsymbol{P} + \boldsymbol{p}')(\boldsymbol{U}_0 + \boldsymbol{u}_0) - \boldsymbol{M}_t(\boldsymbol{P})(\boldsymbol{U}_0) \|,$$

where $\boldsymbol{u}_0$ and $\boldsymbol{p}'$ are perturbation vectors superimposed on the initial value $\boldsymbol{U}_0$ of the basic state $\boldsymbol{U}(t)$ and the parameter $\boldsymbol{P}$, respectively, with $\boldsymbol{u}_0 \in C_\delta$, $\boldsymbol{p}' \in C_\sigma$ as the constraint conditions. By solving Eq. (6), the optimal combined mode of the initial perturbation and parameter perturbation $(\boldsymbol{u}_{0\delta}; \boldsymbol{p}'_\sigma)$ for a given constraint that induces the largest departure from the basic state $\boldsymbol{U}(t)$ at time t is obtained. Mu et al. (2010) still called this optimal combined mode the CNOP, which has two special cases. The first is CNOP-I, denoted by $\boldsymbol{u}_{0\delta,I}$, which is just the previously mentioned CNOP that represents the initial perturbation with the largest nonlinear evolution at the prediction time and is obtained by solving the following optimization problem:

$$J_{\boldsymbol{u}_0}(\boldsymbol{u}_{0\delta,I}) = \max_{\boldsymbol{u}_0 \in C_\delta} \| \boldsymbol{M}_t(\boldsymbol{P})(\boldsymbol{U}_0 + \boldsymbol{u}_0) - \boldsymbol{M}_t(\boldsymbol{P})(\boldsymbol{U}_0) \|. \quad (10)$$

The second case is CNOP-P, denoted by $\boldsymbol{p}'_{\sigma,p}$, which describes the parameter perturbation that results in the largest departure from a given reference state, and which can be obtained by evaluating the following optimization problem:

$$J_p\left(\boldsymbol{p}'_{\sigma,p}\right) = \max_{p' \in C_\sigma} \| \boldsymbol{M}_t(\boldsymbol{P}+\boldsymbol{p}')\left(\boldsymbol{U}_0\right) - \boldsymbol{M}_t(\boldsymbol{P})\left(\boldsymbol{U}_0\right) \|. \quad (11)$$

Physically, the CNOP represents the optimal combined mode of the initial error and the model parameter error. Moreover, the CNOP-I, in perfect model experiments, acts as the optimal initial error, and the CNOP-P, in experiments with perfect initial conditions, represents the optimal parameter error. In their respective scenarios, these cases cause the largest prediction error.

Optimal Model Perturbation: From Linear Tendency Perturbation to Nonlinear Tendency Perturbation

Studies of model errors are related to the second type of predictability problem (Lorenz, 1975). In the section "CONDITIONAL NONLINEAR OPTIMAL PERTURBATION," we reviewed the CNOP-P approach as it relates to model parametric error. However, there exist other sources of model errors, such as uncertainties in external forcing, numerical schemes, model formulation, and so on. Moreover, these kinds of model errors cannot be exactly separated. Therefore, the CNOP-P approach cannot address all kinds of model errors, but only model parametric errors.

Roads (1987) used tendency errors to approximate the combined effect of different kinds of model uncertainties. Following this approach, a forecast model with initial errors and tendency errors can be written as in Eq. (12).

$$\begin{cases} \frac{\partial(\boldsymbol{U}+\boldsymbol{u})}{\partial t} = \boldsymbol{F}(\boldsymbol{U}+\boldsymbol{u}) + \boldsymbol{f}(\boldsymbol{x}, t), \\ \boldsymbol{U}+\boldsymbol{u}\big|_{t=0} = \boldsymbol{U}_0 + \boldsymbol{u}_0, \end{cases} \quad (12)$$

Here, $\boldsymbol{M}_t(\boldsymbol{f})$ is used to denote the propagator of Eq. (12), and $\boldsymbol{M}_t(\boldsymbol{f})$ with $\boldsymbol{f}=0$ is the same as $\boldsymbol{M}_t$ in Eq. (1). Then, we obtain

$$\boldsymbol{M}_t(\boldsymbol{f})(\boldsymbol{U}_0+\boldsymbol{u}_0) = \boldsymbol{U}(\boldsymbol{x}, t) + \boldsymbol{u}_f^I(\boldsymbol{x}, t), \quad (13)$$

where $\boldsymbol{U}(\boldsymbol{x}, t) = \boldsymbol{M}_t(0)(\boldsymbol{U}_0) = \boldsymbol{M}_t(\boldsymbol{U}_0)$. Obviously, $\boldsymbol{u}_f^I(\boldsymbol{x}, t) = \boldsymbol{M}_t(\boldsymbol{f})(\boldsymbol{U}_0+\boldsymbol{u}_0) - \boldsymbol{M}_t(\boldsymbol{U}_0)$, which describes the departure from the basic state $\boldsymbol{U}(\boldsymbol{x}, t)$ (i.e., $\boldsymbol{M}_t(\boldsymbol{U}_0)$) caused by the initial errors $\boldsymbol{u}_0$ and tendency errors $\boldsymbol{f}$. In the scenario, which describes the first type of predictability problem (Lorenz, 1975), the model is thought to be perfect. In this case, the tendency errors are equal to zero (i.e., $\boldsymbol{f}=0$), and the situation in which $\boldsymbol{M}_t(0)(\boldsymbol{U}_0+\boldsymbol{u}_0) = \boldsymbol{U}(\boldsymbol{x}, t) + \boldsymbol{u}(\boldsymbol{x}, t)$ is considered. Here, $\boldsymbol{u}(\boldsymbol{x}, t)$ represents the evolution of initial errors $\boldsymbol{u}_0$. For the second type of predictability problem, the initial fields are assumed to be perfect (i.e., the initial errors $\boldsymbol{u}_0 = 0$), and $\boldsymbol{M}_t(\boldsymbol{f})(\boldsymbol{U}_0) = \boldsymbol{U}(\boldsymbol{x}, t) + \boldsymbol{u}_f(\boldsymbol{x}, t)$ is of interest. Then, $\boldsymbol{u}_f(\boldsymbol{x}, t)$ describes the departure from the basic state $\boldsymbol{U}(\boldsymbol{x}, t)$ caused by the tendency errors $\boldsymbol{f}$, which may describe a type of model systematic error.

(Linear) Optimal Tendency Perturbation

The perturbation evolution equation can be obtained by subtracting Eq. (1) from Eq. (12). Omitting the nonlinear term, a linearized perturbation equation is obtained.

$$\begin{cases} \frac{\partial \boldsymbol{u}}{\partial t} = \boldsymbol{F}'(\boldsymbol{U})\boldsymbol{u} + \boldsymbol{f}(\boldsymbol{x}, t), \\ \boldsymbol{u}\big|_{t=0} = \boldsymbol{u}_0, \end{cases} \quad (14)$$

where $\boldsymbol{u}_0$, $\boldsymbol{u}$, and $\boldsymbol{U}$ have the same meanings as in Eq. (12), and $\boldsymbol{F}'(\boldsymbol{U})$ is the Jacobian of the nonlinear operator $\boldsymbol{F}$ in Eq. (12) with respect to the basic state $\boldsymbol{U}(\boldsymbol{x}, t)$. With the tendency perturbation $\boldsymbol{f}(\boldsymbol{x}, t)$, a maximization problem is defined as follows.

$$\lambda(\boldsymbol{f}^*) = \max_{\boldsymbol{f}} \frac{\| \boldsymbol{L}_t(\boldsymbol{f})(0) \|}{\| \boldsymbol{f} \|}, \quad (15)$$

where $\boldsymbol{L}_t(\boldsymbol{f})$ is the propagator of Eq. (14) and is equivalent to the linear counterpart of the nonlinear propagator $\boldsymbol{M}_t(\boldsymbol{f})$ of Eq. (12). Then the FSV $\boldsymbol{f}^*(\boldsymbol{x})$ proposed by Barkmeijer et al. (2003) can be obtained by solving the Eq. (15) when $\boldsymbol{f}(\boldsymbol{x}, t)$ is constant in time. Meanwhile, if $\boldsymbol{f}(\boldsymbol{x}, t)$ represents time-dependent stochastic processes of Gaussian noise with zero mean for all times and the variances of the variables of interest are cared, then one can obtain the stochastic optimals $\boldsymbol{f}^*(t)$ proposed by Kleeman and Moore (1997) by maximizing the variance of $\| \boldsymbol{L}_t(\boldsymbol{f})(0) \|$ in Eq. (15). Stochastic optimals and FSVs induce significant perturbation growth in linearized models in their respective scenarios.

Obviously, both the stochastic optimal and FSV methods are based on linearized models. Furthermore, Barkmeijer et al. (2003) argued that the stochastic optimal approach was not feasible in a realistic high-dimensional numerical model, whereas the FSV method can avoid this limitation. In particular, Barkmeijer et al. (2003) reported that the FSV represents the fastest-growing constant tendency error in predictability studies. D'Andrea and Vautard (2000) studied similar structures as a way to reduce the systematic error in a quasi-geostrophic model. Farrell and Ioannou (2005) further determined the optimal set of the distributed deterministic and stochastic forcing in forecasting and observation systems over a chosen time interval, also based on a linear system. Despite this progress, the FSV method assumes a linear system and cannot describe the optimal tendency error in nonlinear systems (Duan & Zhao, 2015; Duan & Zhou, 2013).

Nonlinear Forcing Singular Vector

To overcome the limitations of the FSV method, Duan and Zhou (2013) define a nonlinear FSV (NFSV) to describe the optimal tendency errors in nonlinear systems. For a chosen measurement, a tendency perturbation $\boldsymbol{f}_\delta$ is defined as a NFSV if and only if

$$J_\delta(\boldsymbol{f}_\delta) = \max_{\|\boldsymbol{f}\|_a \le \delta} J(\boldsymbol{f}), \quad (16)$$

where

$$J(\boldsymbol{f}) = \| \boldsymbol{M}_t(\boldsymbol{f})(\boldsymbol{U}_0) - \boldsymbol{M}_t(0)(\boldsymbol{U}_0) \|_b, \quad (17)$$

$\|\boldsymbol{f}\|_a \leq \delta$, which is defined by the norm $\|\cdot\|_a$, is the constraint condition of the tendency perturbation $\boldsymbol{f}$. The objective function J with the norm $\|\cdot\|_b$ measures the magnitude of the departure from the basic state $\boldsymbol{M}_\tau(0)(\boldsymbol{U}_0)$ caused by the tendency perturbations. The norms $\|\cdot\|_a$ and $\|\cdot\|_b$ represent different norms. In some situations, the norm $\|\cdot\|_a$ can be the same as $\|\cdot\|_b$ depending on the physical problem being investigated.

The NFSV induces the largest perturbation growth at a given future time τ and considers the effect of nonlinearity. The NFSV can describe the optimal tendency error because of its nonlinearity, but the FSV fails to do it.

The NFSVs are obtained by regarding the constant tendency perturbations as constant tendency errors and evaluating the ones that cause progressively larger prediction errors at prediction time, which may describe model systematic errors that have large effects on prediction results. In this case, the patterns described by the NFSVs may allow to find the regions in which the predictions are most sensitive to model systematic errors; therefore, the corresponding physical processes should be better described by the models. In numerical predictions, one can also determine an optimal external forcing to offset the model uncertainties by assimilating observations in these sensitive regions. In addition, if one takes the constant tendency perturbation as an external forcing with a particular physical meaning, the NFSVs may describe the external forcings to which the weather and climate are significantly sensitive. Furthermore, if the NFSVs are superimposed on an external forcing with a particular physical meaning, they can be used to investigate the effects of the external forcing uncertainties on the prediction results.

Mu et al. (2010) extended the CNOP approach to identify model parameter errors (CNOP-P) that cause the largest prediction error. Actually, if the constant tendency perturbation is expressed as external parameters that display a certain spatial structure, one can use the CNOP-P technique to derive the NFSV. However, this does not mean that the NFSV and CNOP-P are the same. Undoubtedly, there are overlaps between NFSV and CNOP-P, but they are incompatible. Specifically, the NFSV is constant and may include time-independent components of model errors. Therefore, the NFSV may include the effects of the parametric errors that induce time-independent tendency errors, but fails to include the effects of those that induce time-dependent tendency errors, such as parametric errors that are dependent on state variables. Therefore, it is desirable that a time-dependent NFSV approach should be developed, and it is expected to address the effects of all kinds of model errors. Connected with the stochastic optimal approach, one should explore the application of nonlinear stochastic optimal methods in nonlinear stochastic dynamical systems.

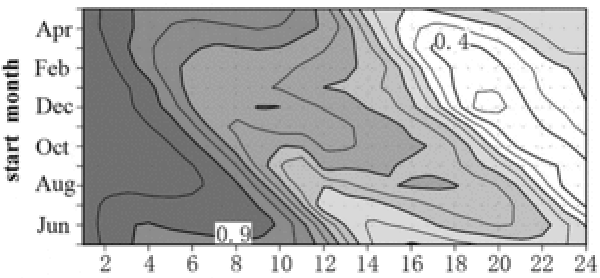

Click to view larger

Figure 1. The SPB Phenomenon. An Niño-3.4 SST anomaly correlation between model ensemble mean predictions and NCEP observations up to a 24-month lead for the period 1982–2004. These are derived from the Scale Interaction Experiment Frontier (SINTEX-F) coupled general circulation model (GCM) and shown as a function of start month and lead time (see Luo et al., 2005). The anomaly correlations decrease quickly during spring. Adapted from Luo et al. (2008).

ENSO Predictability Associated With Initial Errors

As described in the "Introduction," significant progress has been achieved in ENSO theory and predictions, and numerous models have been developed to understand, simulate, and predict ENSO events (Jin, 1997A, 1997B; Kleeman, Moore, & Smith, 1995; McCreary & Anderson, 1991; Wang & Fang, 1996; Zebiak & Cane, 1987), including complex coupled general-circulation models (CGCMs; Palmer et al., 2004; Saha et al., 2006). However, considerable uncertainties still exist in realistic ENSO predictions (Jin et al., 2008; Luo et al., 2008). Furthermore, these models reveal a consistent characteristic of ENSO predictions: if forecasts are made before and through the spring and the beginning of summer, the ENSO predictions tend to be much less successful. This low predictability is the so-called spring predictability barrier (SPB) phenomenon (Figure 1) in ENSO forecasts (Kirtman et al., 2002; Lau & Yang, 1996; McPhaden, 2003; Webster & Yang, 1992). From the perspective of error growth, the SPB referred to here is the phenomenon that ENSO forecasting has a large prediction error; in particular, prominent error growth occurs during the spring when the prediction is made before the spring (see Figure 2; Duan, Xue, & Mu, 2009; Yu, Duan, Xu, & Mu, 2009; Zhang, Duan, & Zhi, 2015). While significant progress has been made in ENSO theories and predictions over the years, especially through the TOGA (Tropical Ocean Global Atmosphere) program (see the review by Wang & Picaut, 2004), considerable SPB phenomena still occur in realistic ENSO predictions and severely reduce the ENSO forecast skill (Duan & Wei, 2012; Jin et al., 2008; Luo et al., 2008; Qi, Duan, Zheng, & Tang, 2016; Zhang et al., 2015).

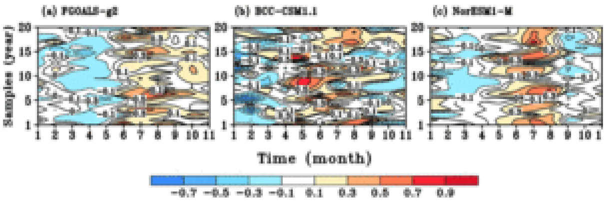

Click to view larger

Figure 2. The ensemble mean of the monthly growth rates of prediction errors of the Niño-3.4 SST for El Niño events in one 20-year SST time series derived from (a) the FGOLAS-g2 (Flexible Global Ocean-Atmosphere-Land System model, Grid-point Version 2); (b) the BCC-CSM1.1 (Beijing Climate Center Climate System Model); and (c) the NorESM1-M (Norwegian Climate Center's Earth System Model). Here, the vertical axes denote the samples of initial errors; the contour lines represent the monthly growth rates of the increase (or decrease) of prediction errors, where the positive (negative) values indicate the growth (decrease) of the prediction errors. The growth rate of prediction errors in a given month was evaluated by subtracting the prediction error in this month from that in the last month. Adapted from Zhang et al. (2015).

The Spring Predictability Barrier for ENSO

The spring predictability barrier (SPB) is a well-known characteristic of ENSO forecasts. The SPB exists not only in coupled models but also in some statistical models (Kirtman et al., 2002). On occasion, the SPB is even stronger in statistical models than in GCMs (van Oldenborgh, Philip, & Collins, 2005). Although many studies have tried to determine the causes of the SPB, agreement has yet to be reached. Some studies argue that the SPB is an intrinsic characteristic of ENSO forecasting because the signal-to-noise ratio for SST tends to be lowest in spring, and even additional observations cannot change the fact of the low signal in spring (Samelson & Tziperman, 2001; Xue, Cane, Zebiak, & Blumenthal, 1994). Other studies describe ENSO as a self-sustaining oscillation, and the model-based prediction of ENSO depends strongly on the initial conditions (Chen, Zebiak, Busalacchi, & Cane, 1995, Chen, Cane, Kaplan, Zebiak, & Huang, 2004; Latif et al., 1998). According to this viewpoint, the SPB arises from the growth of initial errors (Chen et al., 1995, 2004; Duan et al., 2009; Duan & Wei, 2012; Duan & Hu, 2016; Fan, Allen, Anderson, & Balmaseda, 2000; Moore & Kleeman, 1996; Mu, Duan, & Wang, 2007A; Mu, Xu, & Duan, 2007B; Tang, Kleeman, Moore, Weaver, & Vialard, 2003; Xue et al., 1997A, 1997B; Yu et al., 2009; Yu, Mu, & Duan, 2012).

Chen et al. (1995, 2004) proposed a new initialization procedure for El Niño forecasting by considering the coupling between the ocean and the atmosphere during initialization, and they greatly reduced the effect of the SPB on ENSO forecasting and improved the forecast skill of ENSO in the Zebiak-Cane model (Zebiak & Cane, 1987). Webster and Yang (1992) suggested that the annual cycle of the background state of the tropical Pacific, which determines the seasonally varying growth rate, plays an important role in creating the SPB for ENSO (also see Moore & Kleeman, 1996; Thompson & Battisti, 2001). Van Oldenborgh, Burgers, Venzke, Eckert, and Giering (1999) demonstrated that both the phase of the climatological basic state and that of El Niño play important roles in generating the SPB. From these studies, it is known that the SPB is related to three factors: the climatological annual cycle, El Niño itself, and the initial uncertainties. These studies considered either the initial conditions or the El Niño events themselves or the climatological basic state and assume the other two factors remain unchanged. It is conceivable that when the three factors vary freely, the interaction among these factors may significantly influence the SPB. In fact, Mu et al. (2007A) adopted the theoretical WF96 model (Wang & Fang, 1996) and demonstrated that the SPB of El Niño events is a result of the combined effect of the above three factors, which then unifies the viewpoints of the above studies.

Obviously, of the three factors that give rise to the SPB, the former two factors are robustly in existence for ENSO events (Dommenget & Yu, 2016; Stein, Schneider, Timmermann, & Jin, 2010), whereas the third factor is artificial and induced by the limitations of observational instruments, inaccurate initialization of forecast models, and the like. Therefore, even if the seasonality of the annual cycle determined by observation, which is the origin of the seasonal dependence of error growth, is robust in forecast models, particular initial error modes are necessary to cause the SPB. That is, there exists the possibility that some types of initial errors may cause extreme uncertainties in ENSO forecasting through the spring and exhibit a prominent season-dependent evolution related to the SPB because of the seasonality of ocean-atmosphere coupling. Other types of initial errors, however, tend not to yield seasonally dependent evolution of error growth, even though the annual cycle is embedded in the forecast models (Duan et al., 2009; Mu et al., 2007B; Yu et al., 2009). Galanti et al. (2002) and Burgers, Jin, and van Oldenborgh (2005) explored the linear growth of initial errors of ENSO forecasts caused by linear coupled instabilities. In particular, Moore and Kleeman (1996) and Xue et al. (1997A, 1997B), and others, used the LSV approach to identify initial errors that develop quickly and cause a significant SPB for ENSO forecasts. Mu et al. (2003) applied the CNOP approach to the theoretical WF96 model (Wang & Fang, 1996) and showed that nonlinearity can amplify the linear error growth for El Niño events and increase the effect of SPB on the ENSO forecast, finally making the CNOP-type errors be the errors that yield the most significant SPB for El Niño events and, consequently, the largest prediction error. On the other hand, when estimating the optimal growth of prediction errors, the LSV approach tends to underestimate the SPB-induced prediction errors for the nonlinear ENSO. And the CNOP-type errors, since they consider the effect of nonlinearity, are more reasonable for estimating the SPB and related prediction errors, which shows that the CNOP method is superior to the LSV method in describing the initial error that induces the prominent SPB for El Niño (Mu et al., 2007A). Subsequently, Mu et al. (2007B) and Yu et al. (2009) used the Zebiak-Cane model and revealed two types of CNOP-type initial error structures that induce maximal prediction uncertainty and cause the most significant SPB. They noted that CNOP-type initial errors possess a large-scale zonal dipolar pattern of the sea surface temperature anomaly (SSTA) component that is similar to that of the LSV-type initial errors in Xue et al. (1997A, 1997B), but the former covers a broader region than the latter, which leads to a significant difference in their resultant prediction errors and consequently indicates the extreme sensitivity of the prediction results to initial uncertainties. Furthermore, Yu, Mu, and Duan (2012) and Duan and Wei (2012) argued that there exist CNOP-like initial errors in realistic ENSO predictions; particularly, they correspond to larger prediction errors than other initial errors. Therefore, it is reasonable that if one filters the CNOP-like errors in realistic predictions, the SPB may be greatly reduced and the ENSO forecast could be substantially improved.

The studies mentioned in the three preceding paragraphs paid attention to "traditional" EP-El Niño events. Recently, Tian and Duan (2016) adopted a corrected Zebiak-Cane model and showed that the CNOP-type initial errors for CP-El Niño events can also be classified into two types. One type is similar to the EP-El Niño events as shown in Yu et al. (2009), while the second is very different from the EP-El Niño events in Yu et al. (2009) and are associated with a pattern of SSTAs in the central-eastern equatorial Pacific, with a dipole structure of negative anomalies in the east and positive anomalies in the west, and a pattern of thermocline depth anomalies with a slight deepening along the equator. The first type of error leads to a significant SPB for the CP-El Niño, and the second type of error fails to cause an SPB. For EP-type events, both types of CNOP errors, as shown in Yu et al. (2009), cause a significant SPB for tropical SSTA; for CP-type events, only one of the CNOP-type errors induces a significant SPB (Tian & Duan, 2016). This comparison between EP- and CP-El Niño events may show that the EP-El Niño predictions may be much more likely to encounter an SPB than are the CP-El Niño predictions. Hendon et al. (2009) also indicated that the predictive skill of the NIÑO4 index shows much less of an SPB, indicating reduced occurrence of the SPB for CP-El Niño events. From the correlations between the predicted SST and the observed ones obtained by Luo et al. (2008), the NIÑO4 index can also be seen to have a higher prediction skill than the NIÑO3 index, indicating that the CP-El Niño may be much predictable than the EP-El Niño events. Luo et al. (2008) used the SINTEX-F model (Luo et al., 2003; Luo, Masson, Roeckner, Madec, & Yamagata, 2005), which is one of the best models that describe ENSO and have greatly reduced model error. The experiments conducted by Tian and Duan (2016) are based on perfect model predictability experiments. Therefore, we deduce that CP-El Niño is much more predictable than EP-El Niño, if the effect of model errors can be neglected.

Despite the prevalence of studies that have examined the SPB and the many useful results that have been obtained, quite a few questions are still unresolved. In the studies reviewed here thus far, more attention was paid to the tropical Pacific Ocean and initial oceanic conditions received more attention. Given this feature of previous studies, how do the uncertainties occurring in other ocean basins influence ENSO predictions? And what is the role of atmospheric initial conditions and external forcings (such as MJO and WWB) in ENSO predictions? Is oceanic initialization or atmospheric initialization more important in ENSO predictions? What is the role of the coupled initialization in reducing the effects of the SPB? Finally, the most pressing question is: can the SPB be eliminated? All these questions should be urgently addressed, particularly by studies combining theoretical analysis and realistic predictions.

The studies mentioned here on ENSO predictability were based on the assumption that ENSO is a chaotic oscillator. Another hypothesis is that ENSO is a damped, noise-driven oscillator. Recent results on the stability of ENSO also showed evidence favoring the damped, driven oscillator hypothesis (Kim & Jin, 2011; Lübbecke & McPhaden, 2014). Thompson and Battisti (2001) found that the SPB for ENSO also existed in a linear, damped, noise-driven model of intermediate complexity. Furthermore, Levine and Mcphaden (2015) demonstrated that this SPB, like that in the chaotic system, is excited by the annual cycle of the background state of the tropical Pacific (Stein et al., 2010; Stein, Timmermann, Schneider, Jin, & Stuecker, 2014). In the damped system, initial errors are not relevant, and the SPB occurs because of the robust seasonality of the climatological annual cycle. Furthermore, because of the effects of stochastic noise, ENSO must be made up of unpredictable components. In that case, how far ahead can we predict ENSO? The answer may be dependent on the dynamical regimes to which ENSO belongs. Therefore, one should clarify ENSO's regime when addressing the predictability limit for ENSO.

Optimal Precursory Disturbance for ENSO Events

As reviewed in the section "The Spring Predictability Barrier for ENSO," the SPB for ENSO is largely related to initial errors. This indicates that if the forecast systems can exactly capture the initial signal of ENSO, it may have much smaller initial errors and then be favorable for the reduction of the effect of SPB and accurate predictions for ENSO. As such, ones should make it clear which features the initial anomaly signals that evolve into ENSO events most probably. Actually, this question is related to the identification of the source of the predictability for ENSO events. Quite a few scientists adopted optimally growing initial perturbations (or fastest growing initial perturbations) of numerical models to search for the optimal precursor for ENSO events, in attempt to finding the source of ENSO predictability. For example, Xue et al. (1994) realized that the eigenmodes of the linearized version for a numerical model could not be the fastest-growing initial perturbation in non-self-adjoint system and computed the LSVs, finally finding that the fastest growing singular vector evolved into an ENSO event. Palmer et al. (1994) also presented the fastest-growing singular vector that evolves into a structure resembling ENSO with fast growth rate during April. Moore and Kleeman (1996) further investigated nonlinear evolution of singular vectors by use of the intermediate coupled model of Kleeman (1993) and demonstrated that their singular vectors have the potential to develop into ENSO events; furthermore, their singular vectors have structures similar to those described by Xue et al. (1994) and Palmer et al. (1994) and are of the SSTA component with negative anomalies in tropical western Pacific and positive anomalies in tropical eastern Pacific. Thompson (1998) also used LSV to study the characteristic precursor to an ENSO warm event and found similar SSTA patterns for the precursors that lead to ENSO events. Obviously, these studies attempted to use the LSV to identify the optimal precursors for ENSO—that is, the initial anomaly that evolves most probably into an ENSO event. However, the LSVs, by definition, are derived from linearized version of a numerical model. Thus it remains questionable as to whether the LSV can be regarded as the optimal precursors when nonlinearity appears in the ENSO mode. Duan et al. (2004) used a theoretical WF96 model (Wang & Fang, 1996) and demonstrated that the CNOPs (local CNOPs) of annual cycle are quite different from the LSVs in phase space for the long lead times and large amplitude of perturbations; furthermore, their nonlinear and linear evolutions also remained significant differences. Physically, the CNOPs (local CNOPs) of annual cycle were shown to have a robust pattern with negative (positive) Niño-3 SST and positive (negative) thermocline depth anomalies qualitatively; and these patterns evolve into much stronger El Niño (La Niña) event than the LSV-patterns. Duan et al. (2004) therefore regarded these patterns as the optimal precursors of El Niño (La Niña), which are further confirmed by using the NCEP reanalysis data. These optimal precursors of ENSO revealed the observational fact that the thermocline depth displacement takes a phase 3-month lead to SST variation and provided a negative feedback that turns the coupled system from one state to another state. It is obvious that they depict a source of predictability for ENSO—that is, the leading positive (negative) thermocline depth anomalies for El Niño (La Niña). That is to say, if one observes these anomalies in advance, it can be forecasted that an El Niño (La Niña) could occur. If one mirrors the LSV-related precursory disturbance for ENSO shown in previous studies, such as Xue et al. (1994), Palmer et al. (1994) and Moore and Kleeman (1996), to the WF96 model variables and compares them with the CNOP-related precursors, it can be found that the latter presents much earlier signal for ENSO events than the former and favors for the predictions for ENSO events with much longer lead time. Despite the CNOP precursors were resulted from the conceptual WF96 model, they were also confirmed by the results derived by the complex Community Earth System Model (CESM) of the National Center for Atmospheric Research (NCAR; see Duan & Hu, 2016). That is, Duan and Hu (2016) further emphasized the precursory role of the subsurface layer temperature in ENSO onset. Especially, they argued that before the onset of El Niño, the initial positive ocean temperature anomaly first arose in the subsurface layer of warm pool about one year in advance (also see the data analysis results in Li & Mu, 2002).

These studies mainly focused on the tropical Pacific signal of ENSO onset and did not care about those from other ocean basins. In fact, some studies used numerical simulations approach and showed that the ENSO is often influenced by the SST anomalies in the Indian Ocean (Behera & Yamagata, 2003; Luo et al., 2010; Saji & Yamagata, 2003). This indicates that the onset of the ENSO occurring in the tropical Pacific is influenced by not only the initial signals in the tropical Pacific Ocean but also those in the tropical Indian Ocean. Actually, it has been suggested that ENSO predictions generated by either statistical or dynamical model can be improved if the Indian Ocean information is included (Chen & Cane, 2008; Clarke & Van Gorder, 2003; Izumo et al., 2010; Luo et al., 2010). For example, Izumo et al. (2010) improved the forecast skill of ENSO by adopting the corresponding boreal autumn Indian Dipole Mode Index (DMI) and tropical Pacific warm water volume (WWV) as predictors when predicting the El Niño peak during 1981–2009 with a lead time of 14 months. They also extended this conclusion to El Niño forecasting during 1872–2008 (Izumo et al., 2014), and revealed that the Indian DMI is much more helpful in improving ENSO hindcast skills compared with the index of Indian Ocean basin-wide mode, the Indian Monsoon, or the El Niño index itself. These results imply that the predictability of ENSO events is partly from tropical Indian Ocean; furthermore, the atmospheric bridge has been suggested to be a leading contributor to the influence of Indian Ocean on ENSO predictability (Alexander et al., 2002; Annamalai, Liu, & Xie, 2005; Kug & Kang, 2006). Of course, there also exist studies to indicate the role of North Pacific Ocean variability in ENSO predictability sources. Especially, for the new type of CP-El Niño events, Kao and Yu (2009) and Yu and Kim (2011) showed that wind forcing from the subtropical and extratropical atmosphere may play an important role in the occurrence of CP-El Niño events and emphasized that the warming signal for some CP-El Niño events is first from North Pacific. Chen et al. (2015) demonstrated that the diversity of El Niño events results from the random occurrence of westerly wind bursts (WWBs), which may indicate that the source of EP- and CP-El Niño predictability is from westerly wind burst occurring in tropical western Pacific. In any case, the factors that these studies revealed may be more or less related to ENSO predictability source and can act as predictors for ENSO events. However, whether or not these predictors are optimal or most important for ENSO onset forecasts? What is the role of the interactions among Pacific, Indian, even Atlantic oceans’ variabilities in enhancing ENSO predictability? All these remain unknown. To address these questions, optimal methods may be useful. However, it is unclear how to use the optimal methods to identify the optimal predictors for ENSO events and investigate the role of inter-basin coupling in ENSO predictability.

Estimating the Optimal Observing Location for Advancing the Prediction Skill of ENSO Events

The studies discussed in the section associated with SPB for ENSO emphasize that initial errors with particular spatial structures cause much larger prediction errors for ENSO events. Thus, increasing the accuracy of the initial fields provides an effective way to improve the skill of ENSO forecasts. Sufficient observations are required to properly determine the initial fields for the prediction of the ENSO events. Since field observations are costly and will never be dense enough to fully cover the vast space occupied by these events, it is necessary to design an efficient and effective observation strategy, in which one place a limited number of observation stations in specific locations and expects them to have a considerable impact on forecast skills. The “target observation” or “adaptive observation” strategy has been developed to serve this purpose since the 1990s. Its general idea is as follows. To better predict an event at a future time t_1 (the verification time) in a focused area (the verification area), particular areas (sensitive areas) are identified at present time t_d and additional observations are deployed in these areas at a future time t_0 (the target time; $t_d < t_0 < t_1$), where the additional observations are expected to make large contributions to reducing prediction errors at the time t_1 in the verification area (Snyder, 1996). These additional observations are then assimilated by a data assimilation system to form a more reliable initial state, which is then supplied to the model for a more accurate prediction. The target observation strategy has been widely used to improve the forecast skill of weather events, and several field experiments have been successfully implemented to collect target observation (Bergot, 1999; Bishop & Toth, 1999; Palmer, Gelaro, Barkmeijer, & Buizza, 1998; Wu, Chen, Lin, & Chou, 2007). The results for ENSO reviewed in the last section show that ENSO forecasting is sensitive to initial uncertainties, and initial errors with particular structures cause the largest prediction errors for ENSO; furthermore; its main errors are concentrated in particular regions, which indicates that the target observation strategy is also feasible for improving the initial field accuracy for climate event predictions and may provide an effective way to reduce the prediction uncertainties.

The key step in the target observation strategy is to determine the sensitive area for targeting observation; that is, the optimal observing location. Recently, for ENSO events, Yu et al. (2012) demonstrated that the location of CNOP-type initial errors made significant contributions to the prediction uncertainty of EP-El Niño events, and the initial SSTA error arising from the eastern equatorial Pacific tends to grow more significantly than those from other locations for EP-El Niño events; when the initial errors in SSTA in the eastern equatorial Pacific are eliminated, keeping those in other regions unchanged, the prediction errors for EP-El Niño are substantially reduced. This indicates that, if observations in the eastern equatorial Pacific and are increased and assimilated to produce more reliable initial fields, ENSO forecast skill can be greatly improved. Therefore, the eastern equatorial Pacific may represent one of the optimal observing locations for ENSO predictions. In addition, Mu, Yu, Xu, and Gong (2014) emphasized the similarities between the optimal precursors (OPR) and the optimally growing initial errors (OGE) for EP-El Niño events, and noted that the eastern equatorial Pacific can be determined as the optimal observing location for ENSO prediction. Target observations in this area can not only contribute to reduce the effects of initial errors but can also be helpful for identifying the precursor signals for ENSO events to improve ENSO forecast skill.

Based on observation system simulation experiments (OSSEs), Morss and Battisti (2004A, 2004B) suggested that, for ENSO forecasts longer than a few months, the most important area for observations is the eastern equatorial Pacific, south of the equator; a region of secondary importance is the western equatorial Pacific. These sensitive areas are generally consistent with those determined by the CNOP method. Since the CNOP method identifies the most sensitive perturbation, it may put more weight on the most sensitive area for ENSO forecasting, that is, the eastern equatorial Pacific, rather than other areas such as the western equatorial Pacific. More generally, one should further investigate the local CNOPs (, the initial perturbations whose cost function reaches local maximal values at prediction time; see Mu et al., 2003) to identify other sensitive areas for ENSO forecasting. In any case, the sensitive areas identified by Morss and Battisti (2004A, 2004B) serve as verification for the CNOP-estimated sensitivity. By using the sequential importance sampling assimilation method, Kramer and Dijkstra (2013) also showed that the optimal observation locations for SSTs are located in the eastern tropical Pacific for minimizing the uncertainty in the NIÑO3 index, again agreeing with the CNOP results.

All these above studies attempt to identify the optimal locations in which additional observations should be a priority for advancing beyond the SPB and improving El Niño forecast skill. These results focused on the SST component of the initial errors to determine the sensitive area for target observation, and did not consider sufficiently the role of subsurface temperatures in producing the SPB. Recently, Duan and Hu (2016) adopted the concept underlying the CNOP method and studied the target observation for EP-El Niño events by emphasizing the role of oceanic subsurface observations in ENSO predictability using the Community Earth System Model (CESM). They demonstrated that the prediction errors for Niño-3 SSTA are mainly due to the contributions from initial sea surface temperature errors in the regions with large errors in the upper layers of the eastern tropical Pacific and/or in the lower layers of the western tropical Pacific; these regions may represent optimal observational locations for ENSO predictions. Compared with the optimal observational locations determined by the Zebiak-Cane model, the CESM-based study further revealed that subsurface layers of the western tropical Pacific are also particularly important observing locations for EP-El Niño predictions. Hu and Duan (2016) further obtained the OPRs for EP-El Niño and La Niña and showed the similarity between OPRs and the OGEs as identified in the Zebiak-Cane model by Mu et al. (2014). However, comparing the OPRs identified in the two models with each other, the OPRs in the CESM model, due to the influence of the subsurface layer, present a much earlier signal for the occurrence of El Niño and La Niña. Therefore, the OPRs obtained from the CESM model precede those of the Zebiak-Cane model. In addition, the resultant target observations in the sensitive areas identified using the OPRs and OGEs of the CESM model could be helpful for improving the skill of ENSO forecasts with much longer lead times.

For the CP-El Niño events, few studies have examined the predictability of CP-El Niño events, since most climate models only produce EP-El Niño events and fail to produce CP-El Niño events. In an exploratory study, Tian and Duan (2016), as mentioned in section 3.1, used a corrected Zebiak-Cane model to study the predictability of CP-El Niño events. In particular, they identified the CNOP-type initial errors that cause the most significant SPB and then the largest prediction errors and determined the optimal observing locations for advancing beyond the SPB for ENSO. Comparing the results for CP-El Niño events with those for EP-El Niño events shown in Yu et al. (2012), it is found that, for either CP- or EP-El Niño, the CNOP-type initial errors that cause a prominent SPB are concentrated in the eastern tropical Pacific. This may indicate that the prediction uncertainties of both types of El Niño events are most sensitive to the initial errors in the same region. The region may represent a common optimal observing location for the target observation of the two types of El Niño events. The common optimal observing location for the two types of El Niño events forecasting indicates that, when the errors at the optimal observing location are prioritized to be reduced or even eliminated, not only will the prediction errors be reduced substantially, but also models could succeed in predicting the true spatial structure of the two types of El Niño events.

Kramer and Dijkstra (2013) argued that the optimal observation locations for SST are located in the central Pacific for minimizing the uncertainty in the NIÑO4 index, which may indicate that the optimal observing location for CP-El Niño forecasting is located in the central Pacific. This seems not to be consistent with that determined by Tian and Duan (2016). Kramer and Dijkstra (2013) adopted the sequential importance sampling (SIS) method to assimilate the observations for decreasing the spread of ensemble members and used the predictive power index to measure the gain in skill from the pdf produced by the analysis, finally determining the optimal observing locations for ENSO forecasting. Obviously, in the study by Kramer and Dijkstra (2013), the skill of the optimal observations in improving ENSO forecast level is determined by the decrease in the spread among ensemble forecast members, while in Tian and Duan (2016), the skill is measured by reducing prediction errors for ENSO, which corresponds to the difference between forecast results and observations. In an ensemble forecast, an effective ensemble forecast system means that the ratio between the spread and the prediction errors should be approximately equal to 1 (Branković, Palmer, Molteni, Tibaldi, & Cubasch, 1990; Buckingham, Marchok, Ginis, Bothstein, & Rowe, 2010; Eckel & Mass, 2005), which, on the other hand, implies that the possibility exists that the sensitivities measured by the spread and the prediction error are different. This may explain why the optimal observing locations for CP-El Niño events obtained by Tian and Duan (2016) and Kramer and Dijkstra (2013) are different. However, prediction errors measure the distances between predictions and observations and are quite reasonably used to evaluate the sensitivity of the optimal observation method in terms of its ability to improve ENSO forecast skill. Consequently, the optimal observing location for CP-El Niño obtained in Tian and Duan (2016) is much more transparent.

It is also recognized that the optimal observing locations associated with the two types of El Niño obtained here are derived from perfect model predictability experiments and should be further examined in realistic ENSO predictions. In particular, the optimal observing location for CP-El Niño should be further explored by models possessing the ability to reproduce CP-El Niño events. Considering that the onset and evolution of the EP- and CP-El Niño may possess different dynamical and physical mechanisms, the commonality of the optimal observing location associated with the two types of El Niño events remains questionable. Of course, the possibility exists that the two types of El Niño events possess common optimal observing location but different secondarily important observing locations. In any case, the locations for targeting observations associated with the two types of El Niño events should be further explored in depth. A new observation plan named the TPOS (Tropical Pacific Observing System) 2020 has been implemented, which emphasizes the importance of target observation for the two types of El Niño events and provides a good opportunity to study the predictability of the two types of El Niño events (Cravatte et al., 2016). In addition, one should not only identifies the optimal observing location in the ocean but also in the atmosphere for ENSO forecasting; in particular, the role of coupled ocean-atmosphere processes in determining the optimal observing locations for the two types of El Niño should be considered.

ENSO Predictability Associated With Model Errors

Uncertainties in physical parameterizations are a source of model errors (Syu & Neelin, 2000). Zebiak and Cane (1987) and Liu (2002) considered each model parameter and took different values of these parameters to investigate the effect of uncertainties in the parameters on climate simulations and to explore the sensitivity of the climate simulations to the parameter perturbations. Kirtman (1997) found that the ratio of the Rossby radii of deformation in the atmosphere and the ocean has a strong effect on the meridional structure of oceanic Rossby waves, thereby influencing the period of ENSO. MacMynowski and Tziperman (2008) also reported the sensitivity of ENSO's period to various parameters. The results of these studies indicate that parameter uncertainties have an effect on long-term ENSO simulations. However, realistic ENSO predictions focus on short-term climate predictions with lead times from one month to one year, although several ENSO hindcast experiments have employed a lead time of 2 years (Chen et al., 2004; Luo et al., 2008). Furthermore, the multiple parameters of the model may simultaneously have uncertainties, and the method of varying the values of relevant parameters cannot enumerate all combinations of relevant model parameters and explore their effects on the uncertainty associated with ENSO predictability. Additionally, there exist not only model parameter errors but also initial errors in realistic ENSO predictions. To explore predictability in realistic situations, Mu et al. (2010) extended the CNOP approach to include both optimal initial perturbations (CNOP-I) and optimal model parameter perturbations (CNOP-P). This revised CNOP approach is a usable and effective method to search for the optimal combined mode of initial perturbations and model parameter perturbations, and can be used to explore the relative importance of initial errors and parameter errors in yielding substantial prediction errors. Duan and Zhang (2010) and Yu et al. (2012) used the revised CNOP approach and emphasized the important role of initial errors in causing the SPB for EP-El Niño events. In addition, Yu, Mu, and Yu (2014) demonstrated that parameter errors led to neither a noticeable prediction error nor a significant SPB, and had less influence on the prediction uncertainties associated with EP-El Niño. From these studies, it is inferred that initial errors, rather than model parameter errors, are more likely to cause a significant SPB for EP-El Niño events, which emphasizes the importance of data assimilation in El Niño predictions and provides a theoretical basis for ENSO target observations.

Gebbie and Tziperman (2009) found that implementation of WWBs improves predictions of the onset and development of the exceptionally large 1997 El Niño event, suggesting the potential for improving ENSO predictions during the SPB. In addition, Lopez and Kirtman (2014) showed that including state-dependent WWBs in a fully coupled prediction model significantly increased ENSO prediction skill. These two studies indicate that when the model lacks the effect of WWBs and yields model errors, the ENSO forecast skill is also significantly influenced. In particular, Yu, Weller, and Liu (2003) suggested that the characteristics of WWBs depend on the large-scale SST field and are therefore not purely stochastic, which implies that the model errors induced by the lack of WWBs may have a certain structure and thus have a large effect on prediction errors for ENSO. It is clear that, in realistic ENSO predictions, the prediction errors are generally caused by not only initial errors but also model errors (Blanke, Neelin, & Gutzler, 1997; Flügel & Chang, 1998; Hao & Ghil, 1994; Latif et al., 1998; Liu, 2002; Williams, 2005; Wu, Anderson, & Davey, 1993; Yu & Kim, 2010; Zavala-Garay, Moore, & Kleeman, 2004; Zhang, Zebiak, Kleeman, & Keenlyside, 2003); furthermore, the model errors may exhibit patterns reflecting a particular structure.

Kleeman and Moore (1997) explored the effects on ENSO predictability due to stochastic atmospheric transients using the stochastic optimal approach. They showed that the sensitivity of ENSO predictability to forcing is greatest during the northern spring season and prior to warm events, and that a *western* Pacific dipole pattern in heat flux noise is most efficient in forcing *eastern* Pacific SST variance; in particular, they demonstrated that the noise projects predominantly onto the dominant stochastic optimal, and in addition, approximately 95% of the error growth can be attributed to stochastic forcing with a strong synoptic component. These results also indicate that model error having a particular pattern would induce large prediction errors for ENSO, which supports the viewpoint of Yu et al. (2003). Moore and Kleeman (1999) demonstrated that the stochastic optimal noise forcing produces perturbations in the system that grow rapidly, and the response of the system to the stochastic optimals is to induce perturbations that bear a strong resemblance to the westerly and easterly wind bursts frequently observed in the western tropical Pacific, which, in the model, acted as efficient precursors for ENSO episodes. Moore et al. (2006) demonstrated that the optimal forcing patterns characterized by stochastic optimal are remarkably similar to those described by the FSV method and to the dominant singular vectors computed in a previous related study. Therefore, they suggest that, irrespective of whether the forcing is in the form of an impulse, is time invariant, or is stochastic in nature, the optimal excitation for the eigenmode that describes ENSO in each model is the same. It may indicate that the optimal forcing characterized by stochastic optimal is equivalent to that derived using the FSV method, at least for ENSO.

Model errors are produced by not only uncertainties in model parameters, but also by unrecognized physical processes and atmospheric noise, etc. Furthermore, the effects of these kinds of model errors on ENSO predictability are mixed and cannot be exactly separated. Therefore, one has to explore the combined effects of the different kinds of model errors to provide information useful for improving prediction skill. In fact, the FSV method is often used to describe the optimal tendency error, which reflects combined effect of kinds of model errors and causes the largest prediction error (Barkmeijer et al., 2003). However, the FSV method is established on a linear dynamical system frame and cannot fully consider effect of nonlinearity. Then Duan and Zhao (2015) used the NFSV approach (the generalization of the FSV method) and studied the combined effect of different kinds of model errors to identify the most disturbing tendency error of the Zebiak-Cane model associated with El Niño predictions and presented the spatial distribution of tendency error that contributes most to the prediction uncertainties of EP-El Niño prediction. They found that the most disturbing tendency errors associated with EP-El Niño events often present a structure different from that described by the FSV method and often concentrate the tendency errors with large values in a few areas, which indicate that the model errors in these areas make much larger contributions to the occurrence of prediction errors. Duan et al. (2014) superimposed an external forcing term generated using an optimal forcing vector approach to the model tendency and corrected the model simulation closest to the observational data, reproducing the observed ENSO events. The results shown in Duan, Zhao, and Hu (2016) suggest that if one assimilates the observational data to determine an external forcing term and make the model simulation closest to the observational data in the area where the model tendency errors concentrate beforehand, the corrected model may generate much more skillful forecasts for ENSO than do it in other regions. In particular, what is more interesting is that the most disturbing tendency error associated with EP-El Niño predictions shows considerable similarities with the CNOP-type initial errors in Yu et al. (2012; Figure 3). Regarding the regions provided by the CNOP sensitivity as optimal observing locations for EP-El Niño events, the similarities between the CNOP-type initial errors and the NFSV-type tendency errors may show that the ENSO prediction errors are most sensitive to not only the initial errors in the sensitive area but also the model errors in this area. Therefore, we infer that increasing the density of observations collected in this sensitive area will help us to not only decrease the initial uncertainties to improve ENSO forecast skill, but also understand the dynamical mechanism of El Niño events and then improve models.

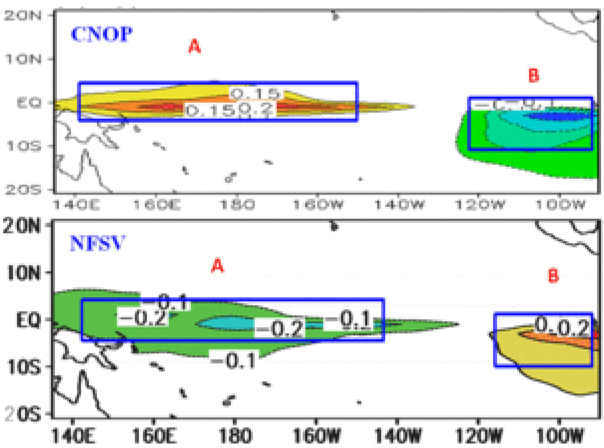

Click to view larger

Figure 3. The SSTA component of CNOP-type initial error (Yu et al., 2012) and NFSV-type tendency error obtained by the Zebiak-Cane model (Duan & Zhao, 2015). Regions A and B represent the sensitive areas for targeting SST observations associated with ENSO predictions.

For CP-El Niño events, most models fail to simulate CP-El Niño events, which may cause few studies to explore their predictability from an error growth viewpoint. In particular, the authors are unaware of any paper that explores the effects of model error on the predictability of CP-El Niño events from an error growth viewpoint. Therefore, there exist many unresolved questions regarding the predictability of CP-El Niño events. For example, what is the tendency error (in the scenario of chaotic ENSO) or the stochastic forcing (in the scenario of damped and noise-driven ENSO) that has the largest effect on prediction uncertainties for CP-El Niño events? What is the relationship between the optimal initial error and tendency error or stochastic optimal forcing? And what useful information on increasing forecast skill can be provided by the optimal tendency error or stochastic optimal for CP-El Niño events? Finally, for EP- and CP-El Niño events, which physical process is responsible for the most disturbing tendency error or stochastic forcing? Can one obtain insight into the climatological conditions for the two types of El Niño events, especially CP-El Niño events? In any case, it is expected that future ENSO studies will lead to improved skill in predicting which types of El Niño events will occur.

Summary and Discussion

In examining traditional optimization methods (such as the LSV, stochastic optimal, and FSV methods) for exploring the predictability of ENSO events with reference to initial errors and model errors predictability, it becomes clear that the traditional methods are often based on linearized dynamical systems and present linear approximations to nonlinear ones; therefore, they do not enable us to fully consider the effects of nonlinear physical processes on predictability. Reviewing the results obtained using traditional methods demonstrates the usefulness of newly developed nonlinear techniques, especially the CNOP and NFSV methods, in characterizing the predictability of ENSO events with reference to initial errors and model errors. For the ENSO predictability caused by initial errors, the “spring predictability barrier” (SPB) for ENSO, based on several studies, is shown to result from the combined effects of the climatological annual cycle, the ENSO events themselves, and the initial error structures. In particular, there is an emphasis on the role of particular initial error patterns in causing a significant SPB. CNOP-type initial errors, compared with other types of initial errors, such as linear singular vector (LSV)–type initial errors, cause much more significant SPB for ENSO events and present more sensitivity to ENSO predictions. This also sheds light on the fact that the CNOP is superior to the LSV in demonstrating the SPB, especially the effect of nonlinearity on SPB for ENSO. Then, based on a review of studies of target observations for ENSO forecasting, it seems that the CNOP approach is superior to the LSV approach in identifying the optimal observing locations associated with target observations; however, the results from the CNOP and OSSE methods are generally similar, giving credibility to the sensitive areas identified. Furthermore, it is possible that the diversity of ENSO does not influence the optimal observing locations. From the results mentioned here, it could be concluded that the CP-El Niño events, in situations in which model error effects can be neglected, may be more predictable than EP-El Niño events because of the SPBs' much weaker sensitivities to initial uncertainties. Together with the optimal observing locations for the two types of El Niño events identified here, this result can then provide guidance for ongoing and planned observation networks, including TPOS-2020.

For the effects on ENSO predictability associated with model errors, different studies have shown that model errors with a particular structure have a significant effect on prediction uncertainties for ENSO; furthermore, these studies show that the optimal tendency errors or optimal forcing noise present a structure similar to that of the optimal initial error, which may indicate that the prediction errors for ENSO are most sensitive to not only the initial error with a particular structure but also the model tendency error having a similar structure. If using such optimal initial errors to determine the initial sensitivity and the optimal observing locations for ENSO forecasting, the model errors occurring in the optimal locations have the most significant effect on ENSO forecast uncertainties. As such, one can use the additional observations in the optimal locations to optimize not only the initial fields but also the model behavior.

In spite of the considerable progress that has been made, the results described here still need much more work to validate their accuracy. In addition to these, other studies are also required to further our understanding of the complexity of the ENSO events and their predictability. Most of the presently obtained results on predictability limits may only be applicable to the stationary EP-El Niño events, and future works should make further contributions to account for the uncertainties of ENSO forecast caused by the CP-El Niño events, as well as by global warming and its recent hiatus. On February 6–8, 2013, a workshop on ENSO diversity was held by CLIVAR in Boulder, Colorado, and a report was published (U.S. CLIVAR Project Office, 2013). This report noted the outstanding issues and research priorities. One of the major issues is the diversity of ENSO and the related predictability limit.

In addition, the results presented here are mainly derived from data confined to the tropical Pacific. However, quite a few studies indicated that various regions outside the tropical Pacific regions, such as the North Pacific (Kim, Yu, Kumar, & Wang, 2012; Yu & Kim, 2011), South Pacific (Zhang, Clement, & Di Nezio, 2014), Indian (Yuan, Zhou, & Zhao, 2013; Zhou, Duan, Mu, & Feng, 2015) and Atlantic Oceans (Boschat, Terray, & Masson, 2013), as well as local atmospheric noise (e.g., westerly wind bursts [WWBs]; Chen et al., 2015; Fedorov, Hu, Lengaigne, & Guilyardi, 2015) can excite ENSO events of different types. Therefore, the uncertainties existing in other ocean basins should also be investigated in terms of their effects on ENSO predictability. Meanwhile, uncertainties arising from the atmosphere and the coupling between the ocean and the atmosphere are especially of concern for ENSO predictability.

From the studies that have been reviewed here, it is known that the LSV, CNOP, stochastic optimal, FSV, and NFSV approaches are, in the early 21st century, being used to consider the uncertainties of either oceanic or atmospheric variables with common timescales. As mentioned in the "INTRODUCTION," ENSO arises from the coupling between ocean and atmosphere. However, the related oceanic and atmospheric motions display very different timescales; but they interact with each other and strongly influence weather and climate, especially through ENSO. Consequently, these approaches have to address the issues on the different scales that ocean and atmosphere present in initialization. Similar issues also occur in variational data assimilation, but they present challenges in exploring how to resolve it. In addition, these approaches, by definition, have to depend on the models used. Especially for the parameter errors or tendency errors, model dependence can be particularly severe. Despite some of the conclusions reviewed here have shown to be robust in different models, there exist some results that should be further examined in other models. It is expected that useful information for improving ENSO forecast skill can be provided and applicable to most of the ENSO forecast systems.

Studies of the predictability of ENSO are challenging. Studies of predictability of ENSO are multidisciplinary in nature, requiring collaboration among different fields of science, including meteorology, oceanography, mathematics, and physics. The work presented here shows considerable promise, and there is every reason to believe that more exciting progress is yet to come that will significantly improve the accuracy of ENSO forecasts and thus disaster prevention, climate change mitigation, and sustainable socioeconomic development (Mu, Duan, Chen, & Yu, 2015).

Acknowledgments

This work was jointly sponsored by the National Natural Science Foundation of China (Grant nos. 41230420 and 41525017).

References

Alexander, M. A., Blade, I., Newman, M., Lanzante, J. R., Lau, N. C., & Scott, J. D. (2002). The atmospheric bridge: The influence of ENSO teleconnections on air-sea interaction over the global oceans. *Journal of Climate*, *15*, 2205–2231.

Annamalai, H., Liu, P., & Xie, S. P. (2005). Southwest Indian Ocean SST variability: Its local effect and remote influence on Asian monsoons. *Journal of Climate*, *18*, 4150–4167.

Ashok, K., Behera, S. K., Rao, S. A., Weng, H. Y., & Yamagata, T. (2007). El Niño Modoki and its possible teleconnection. *Journal of Geophysical Research*, *112*, C11007.

Barkmeijer, J., Iversen, T., & Palmer, T. N. (2003). Forcing singular vector and other sensitivity model structures. *Quarterly Journal of Royal Meteorological Society*, *129*, 2401–2423.

Behera, S. K., & Yamagata, T. (2003). Influence of the Indian Ocean dipole on the southern oscillation. *Journal of the Meteorological Society of Japan*, 2nd series, *81*(1), 169–177.

Bergot, T. (1999). Adaptive observations during FASTEX: A systematic survey of upstream flights. *Quarterly Journal of the Royal Meteorological Society*, *125*, 3271–3298.

Bishop, C. H., & Toth, Z. (1999). Ensemble transformation and adaptive observations. *Journal of the Atmospheric Sciences*, *56*, 1748–1765.

Bjerknes, J. (1969). Atmospheric teleconnections from the equatorial pacific. *Monthly Weather Review*, *97*, 163–172.

Blanke, B., Neelin, J. D., & Gutzler, D. (1997). Estimating the effect of stochastic wind stress forcing on ENSO irregularity. *Journal of Climate*, *10*, 1473–1486.

Boschat, G., Terray, P., Masson, S. (2013). **Extratropical forcing of ENSO**. *Geophysical Research Letters*, *40*, 1605–1611.

Branković, Č., Palmer, T. N., Molteni, F., Tibaldi, S., & Cubasch, U. (1990). Extended-range predictions with ECMWF models: Time-lagged ensemble forecasting [J]. *Quarterly Journal of the Royal Meteorological Society*, *116*, 867–912.

Buckingham, C., Marchok, T., Ginis, I., Bothstein, L., & Rowe, D. (2010). Short- and medium-range prediction of tropical and transitioning cyclone tracks within the NCEP global ensemble forecasting system. *Weather Forecasting*, *25*, 1736–1754.

Burgers, G., Jin, F. F., & van Oldenborgh, G. J. (2005). **The simplest ENSO recharge oscillator**. *Geophysical Research Letter*, *32*, L13706.

Cane, M. A. (1983). Oceanographic events during El Niño. *Science*, *222*, 1189–1195.

Chen, D., & Cane, M. A. (2008). El Niño prediction and predictability. *Journal of Computational Physics*, *227*, 3625–3640.

Chen, D., Cane, M. A., Kaplan, A., Zebiak, S. E., & Huang, D. J. (2004). Predictability of El Niño over the past 148 years. *Nature*, *428*, 733–736.

Chen, D., Lian, T., Fu, C., Cane, M. A., Tang, Y., Murtugudde, R., . . . Zhou, L. (2015). **Strong influence of westerly wind bursts on El Niño diversity**. *National Geoscience*, *8*, 339–345.

Chen, D. K., Zebiak, S. E., Busalacchi, A. J., & Cane, M. A. (1995). An improved procedure for El Niño forecasting: Implications for predictability. *Science*, *269*, 1699–1702.

Clarke, A. J., & Van Gorder, S. (2003). Improving El Niño prediction using a space-time integration of Indo-Pacific winds and equatorial Pacific upper ocean heat content. *Geophysical Research Letters*, *30*, 1399.

Cravatte, S., Kessler, W. S., Smith, N., Wijffels, S. E., et al. (2016). First Report of Tropical Pacific Observing System 2020. Global Ocean Observing System-215, 220 pp. Available **online**.

D'Andrea, F., & Vautard, R. (2000). Reducing systematic errors by empirically correcting model errors. *Tellus A: Dynamic Meteorology and Oceanography*, *52*, 21–41.

Dewitte, B, Choi, J., An, S. I., & Thual, S. (2012). Vertical structure variability and equatorial waves during central Pacific and eastern Pacific El Niños in a coupled general-circulation model. *Climate Dynamics*, *38*, 2275–2289.

Ding, H., Keenlyside, N., Latif, M., Park, W., & Wahl, S. (2015). The impact of mean state errors on equatorial Atlantic interannual variability in a climate model. *Journal of Geophysical Research: Oceans*, *120*, 1133–1151.

Dommenget, D., & Yu, Y. (2016). **The seasonally changing cloud feedbacks contribution to the ENSO seasonal phase-locking**. *Climate Dynamics*, *47*, 3661–3672.

Duan, W., & Hu, J. (2016). The initial errors that induce a significant "spring predictability barrier" for El Niño events and their implications for target observation: Results from an earth system model. *Climate Dynamics*, *46*, 3599–3615.

Duan W. S., Liu, X. C., Zhu, K. Y., & Mu, M. (2009). **Exploring the characteristic of initial errors that cause a significant "spring predictability barrier" for El Niño events**. *Journal of Geophysical Research*, *114*, C04022.

Duan, W. S., & Mu, M. (2009). **Conditional nonlinear optimal perturbation: Applications to stability, sensitivity, and predictability**. *Science in China Series D: Earth Sciences*, *52*(7), 883–906.

Duan, W. S., Mu, M., & Wang, B. (2004). **Conditional nonlinear optimal perturbations as the optimal precursors for El Niño–Southern Oscillation events**. *Journal of Geophysical Research: Atmosphere*, *109*(D23), 105.

Duan, W. S., Tian, B., & Xu, H. (2014). Simulations of two types of El Niño events by an optimal forcing vector approach. *Climate Dynamics*, *43*, 1677–1692.

Duan, W. S., & Wei, C. (2012). **The "spring predictability barrier" for ENSO predictions and its possible mechanism: Results from a fully coupled model**. *International Journal Climatology*, *33*, 1280–1292.

Duan, W. S., Xue, F., & Mu, M. (2009). Investigating a nonlinear characteristic of ENSO events by conditional nonlinear optimal perturbation. *Atmospheric Research*, *94*, 10–18.

Duan W. S., & Zhang, R. (2010). Is model parameter error related to a significant spring predictability barrier for El Niño events? Results from a theoretical model. *Advances in Atmospheric Science*, *27*, 1003–1013.

Duan, W. S., & Zhao, P. (2015). Revealing the most disturbing tendency error of Zebiak-Cane model associated with El Niño predictions by nonlinear forcing singular vector approach. *Climate Dynamics*, *44*, 2351–2367.

Duan, W. S., Zhao, P., & Hu, J. Y. (2016). **The role of model errors represented by nonlinear forcing singular vector-type tendency error in causing the "spring predictability barrier" for ENSO predictions**. *Journal of Meteorological Research*., *30*(6), 853–866.

Duan, W. S., & Zhou, F. F. (2013). **Nonlinear forcing singular vector of a two-dimensional quasi-geostrophic model**. *Tellus A: Dynamic Meteorology and Oceanography*, *65*(1), 18452.

Eckel, F. A., & Mass, C. (2005). Aspects of effective mesoscale, short-range ensemble forecasting. *Weather Forecasting*, *20*, 328–350.

Fan, Y., Allen, M. R., Anderson, D. L. T., & Balmaseda, M. A. (2000). How predictability depends on the nature of uncertainty in initial conditions in a coupled model of ENSO. *Journal of Climate*, *13*, 3298–3313.

Farrell, B., & Ioannou, P. J. (2005). Distributed forcing of forecast and assimilation systems. *Journal of the Atmospheric Sciences*, *62*, 460–475.

Fedorov, A. V., Hu, S. N., Lengaigne, M., & Guilyardi, E. (2015). The impact of westerly wind bursts and ocean initial state on the development, and diversity of El Niño events. *Climate Dynamics*, *44*, 1381–1401.

Fedorov, A. V., & Philander, S. G. (2000). Is El Niño changing? *Science*, *288*, 1997–2002.

Flügel, M., & Chang, P. (1998). Does the predictability of ENSO depend on the seasonal cycle? *Journal of the Atmospheric Sciences*, *55*, 3230–3243.

Galanti, E., Tziperman, E., Harrison, M., Rosati, A., Giering, R., & Sirkes, Z. (2002). The equatorial thermocline outcropping: A seasonal control on the tropical Pacific ocean-atmosphere instability strength. *Journal of Climate*, *15*, 2721–2739.

Gebbie, G., & Tziperman, E. (2009). Predictability of SST-modulated westerly wind bursts. *Journal of Climate*, *29*, 3894–3909.

Ham, Y. G., & Kug, J. S. (2012). How well do current climate models simulate two types of El Niño? *Climate Dynamics*, *39*, 383–398.

Ham, Y. G., Sung, M. K., An, S. I., Schubert, S., & Kug, J. S. (2014). Role of tropical Atlantic SST variability as a modulator of El Niño teleconnections. *Journal of the Atmospheric Sciences*, *50*, 247–261.

Hao, Z., & Ghil, M. (1994). Data assimilation in a simple tropical ocean model with wind stress errors. *Journal of Physical Oceanography*, *24*, 2111–2128.

Hawkins, E., & Sutton, R. (2009). **The potential to narrow uncertainty in regional climate predictions**. *Bulletin of the American Meteorological Society*, *92*, 1181–1192.

Hendon, H. H., Lim, E., Wang, G., Alves, O., & Hudson, D. (2009). **Prospects for predicting two flavors of El Niño**. *Geophysical Research Letters*, *36*, L19713.

Hoerling, M. P., Kumar, A., & Zhong, M. (1997). El Niño, La Niña, and the nonlinearity of their teleconnections. *Journal of Climate*, *10*, 1769–1786.

Hu, J. Y., & Duan, W. S. (2016). **Relationship between optimal precursory disturbances and optimally growing initial errors associated with ENSO events: Implications to target observations for ENSO prediction**. *Journal of Geophysical Research: Oceans*, *121*, 2901–2917.

Izumo, T., Lengaigne, M., Vialard, J., Luo, J. J., Yamagata, T., & Madec, G. (2014). Influence of Indian Ocean dipole and Pacific recharge on following year's El Niño: Interdecadal robustness. *Climate Dynamics*, *42*, 291–310.

Izumo, T., Vialard, J., Lengaigne, M., Montégut, C. D. B., Behera, S. K., Luo, J. J., . . . Yamagata, T. (2010). Influence of the state of the Indian Ocean dipole on the following year's El Niño. *Nature Geoscience*, *3*, 168–172.

Jeong, H. I., Lee, D. Y., Ashok, K., Ahn, J. B., Lee, J. Y., Luo, J. J., . . . Ham, Y. G. (2012). Assessment of the APCC coupled MME suite in predicting the distinctive climate impacts of two flavors of ENSO during boreal winter. *Climate Dynamics*, *39*, 475–493.

Jin, E. K., Kinter, J. L., III, Wang, B., Park, C.-K., Kang, I.-S., Kirtman, B. P., . . . Yamagata, T. (2008). Current status of ENSO prediction skill in coupled ocean–atmosphere models. *Climate Dynamics*, *31*, 647–664.

Jin, F. F. (1997a). An equatorial ocean recharge paradigm for ENSO. Part I: Conceptual model. *Journal of the Atmospheric Sciences*, *54*, 811–829.

Jin, F. F. (1997b). An equatorial ocean recharge paradigm for ENSO. Part II: A stripped-down coupled model. *Journal of the Atmospheric Sciences*, *54*, 830–847.

Kao, H. Y., & Yu, J. Y. (2009). Contrasting Eastern-Pacific and Central-Pacific types of ENSO. *Journal of Climate*, *22*, 615–632.

Kim, S. T., & Jin, F. F. (2011). An ENSO stability analysis. Part I: results from a hybrid coupled model. *Climate Dynamics*, *36*, 1593–1607.

Kim, S. T., Yu, J. Y., Kumar, A., & Wang, H. (2012). Examination of the two types of ENSO in the NCEP CFS model and its extratropical associations. *Monthly Weather Review*, *140*, 1908–1923.

Kirtman, B. P. (1997). Oceanic Rossby wave dynamics and the ENSO period in a coupled model. *Journal of Climate*, *10*, 1690–1705.

Kirtman, B., Power, S. B., Adedoyin, J. A., Boer, G. J., Bojariu, R., Camilloni, I., . . ., Wang, H. J. (2013). Near-term Climate Change: Projections and Predictability. In: *Climate Change 2013: The Physical Science Basis* (pp. 953–1028). Contribution of Working Group I to the Fifth Assessment Report of the Intergovernmental Panel on Climate Change [T. F. Stocker, D. Qin, G.-K. Plattner, M. Tignor, S. K. Allen, J. Boschung, A. Nauels, Y. Xia, V. Bex, & P. M. Midgley (Eds.)]. Cambridge, UK and New York: Cambridge University Press.

Kirtman, B. P., & Schopf, P. S. (1998). Decadal variability in ENSO predictability and prediction. *Journal of Climate*, *11*, 2804–2822.

Kirtman, B. P., Shukla, J., Balmaseda, M., Graham, N., Penland, C., Xue, Y., & Zebiak, S. (2002). Current status of ENSO forecast skill: A report to the Climate Variability and Predictability Numerical Experimentation Group. CLIVAR Working Group on Seasonal to Interannual Prediction. International CLIVAR Project Office, CLIVAR Publication Series No. 56, 26p.

Kleeman, R. (1993). On the dependence of hindcast skill on ocean thermodynamics in a coupled ocean–atmosphere model. *Journal of Climate*, *6*, 2012–2033.

Kleeman, R., & Moore, A. M. (1997). A theory for the limitation of ENSO predictability due to stochastic atmospheric transients. *Journal of Atmospheric Sciences*, *54*, 753–767.

Kleeman, R., Moore, A. M., & Smith, N. R. (1995). Assimilation of subsurface thermal data into an intermediate tropical coupled ocean–atmosphere forecast model. *Monthly Weather Review*, *123*, 3103–3113.

Kramer, K., & Dijkstra, H. A. (2013). Optimal localized observations for advancing beyond the ENSO predictability barrier. *Nonlinear Processes in Geophysics*, *20*, 221–300.

Kug, J. S., Ham, Y. G., Lee, J. Y., & Jin, F. F. (2012). **Improved simulation of two types of El Niño in CMIP5 models**. *Environmental Research Letters*, *7*(2012), 034002.

Kug, J. S., Jin, F. F., & An, S. I. (2009). Two types of El Niño events: Cold tongue El Niño and warm pool El Niño. *Journal of Climate*, *22*, 1499–1515.

Kug, J. S., & Kang, I. S. (2006). Interactive feedback between ENSO and the Indian Ocean. *Journal of Climate*, *19*, 1784–1801.

Larkin, N. K., & Harrison, D. E. (2005). On the definition of El Niño and associated seasonal average US weather anomalies. *Geophysical Research Letters*, *32*, L13705.

Latif, M., Anderson, D., Barnett, T., Cane, M., Kleeman, R., Leetmaa, A., . . . Schneider, E. (1998). A review of the predictability and prediction of ENSO. *Journal of Geophysical Research: Oceans*, *103*(C7), 14375–14393.

Latif, M., Barnett, T. P., Cane, M. A., Flugel, M., Graham, N. E., Vonstorch, H., . . . Zebiak, S. E. (1994). A review of ENSO prediction studies. *Climate Dynamics*, *9*, 167–179.

Lau, K. M., & Yang, S. (1996). The Asian monsoon and predictability of the tropical ocean-atmosphere system. *Quarterly Journal of the Royal Meteorological Society*, *122*, 945–957.

Levine, A. F. Z., & McPhaden, M. J. (2015). **The annual cycle in ENSO growth rate as a cause of the spring predictability barrier**. *Geophysical Research Letters*, *42*, 5034–5041.

Li, C. Y., & Mu, M. Q. (2002). A further study of the essence of ENSO, *Chinese Journal of Atmospheric Sciences*, *26*, 309–328.

Liu, Z. (2002). A simple model study of ENSO suppression by external periodic forcing. *Journal of Climate*, *15*, 1088–1098.

Lopez, H., & Kirtman, K. P. (2014). WWBs, ENSO predictability, the spring barrier and extreme events. *Journal of Geophysical Research: Atmosphere*, *119*, 10114–10138.

Lorenz, E. N. (1962a). Simplified dynamic equations applied to the rotating-basin experiments. *Journal of Atmospheric Sciences*, *19*, 39–51

Lorenz, E. N. (1962b). The statistical prediction of solutions of dynamic equations. *Proceedings of the International Symposium on Numerical Weather Predictions, Tokyo: Japan Meteorological Society*, *647*, 629–635.

Lorenz, E. N. (1963). Deterministic nonperiodic flow. *Journal of Atmospheric Sciences*, *20*, 131–140.

Lorenz, E. N. (1965). A study of the predictability of a 28-variable model. *Tellus*, *17*, 321–333.

Lorenz, E. N. (1969). The predictability of a flow which possesses many scales of motion. *Tellus*, *21*, 289–307.

Lorenz, E. N. (1975). Climatic predictability in the physical basis of climate and climate modeling (Report, GARP Publications Series No. 16, pp. 132–136). World Meteorological Organization, Geneva, Swiss Confederation.

Lu, J. X., & Hsieh, W. W. (1998). On determining initial conditions and parameters in a simple coupled atmosphere-ocean model by adjoint data assimilation. *Tellus A: Dynamic Meteorology and Oceanography*, *50*, 534–544.

Luo, J. J., Masson, S., Behera, S. K., Swadhin, D. P., Gualdi, S., Navarra, A., & Yamagata, T. (2003). **South Pacific origin of the decadal ENSO-like variation as simulated by a coupled GCM**. *Geophysical Research Letters*, *30*(24), 2250.

Luo, J. J., Masson, S., Behera, S. K., & Yamagata, T. (2008). Extended ENSO predictions using a fully coupled ocean-atmosphere model. *Journal of Climatology*, *21*, 84–93.

Luo, J. J., Masson, S., Roeckner, E., Madec, G., & Yamagata, T. (2005). Reducing climatology bias in an ocean-atmosphere CGCM with improved coupling physics. *Journal of Climatology*, *18*, 2344–2360.

Luo, J. J., Zhang, R., Behera, S. K., Masumoto, Y., Jin, F. F., Lukas, R., & Yamagata, T. (2010). Interaction between El Niño and extreme Indian Ocean dipole. *Journal of Climate*, *23*, 726–742.

Lübbecke, J. F., & McPhaden, M. J. (2014). Assessing the 21st century shift in ENSO variability in terms of the Bjerknes stability index. *Journal of Climate*, *27*, 2577–2587.

Macmynowski, D. G., & Tziperman, E. (2008). Factors affecting ENSO's period. *Journal of Atmospheric Sciences*, *65*, 1570–1586.

McCreary, J. P., & Anderson, D. L. T. (1991). An overview of coupled ocean-atmosphere models of El Niño and the Southern Oscillation. *Journal of Geophysical Research*, *96*, 3125–3150.

McPhaden, M. J. (2003). **Tropical Pacific Ocean heat content variations and ENSO persistence barriers**. *Geophysical Research Letters*, *30*, 1480.

McPhaden, M. J., Zebiak, S. E., & Glantz, M. H. (2006). ENSO as an integrating concept in earth science. *Science*, *314*, 1740–1745.

Moore, A. M., & Kleeman, R. (1996). The dynamics of error growth and predictability in a coupled model of ENSO. *Quarterly Journal of the Royal Meteorological Society*, *122*, 1405–1446.

Moore, A. M., & Kleeman, R. (1999). Stochastic forcing of ENSO by the intraseasonal oscillation. *Journal of Climate*, *12*, 1199–1220.

Moore, A., Zavala-Garay, J., Tang, Y. M., Kleeman, R., Weaver, A. T., Vialard, J., . . . Fisher, M. (2006). **Optimal forcing patterns for coupled models of ENSO**. *Journal of Climate*, *19*, 4683–4699.

Morss, R. E., & Battisti, D. S. (2004a). Designing efficient observing networks for ENSO prediction. *Journal of Climate*, *17*, 3074–3089.

Morss, R. E., & Battisti, D. S. (2004b). Evaluating observing requirements for ENSO prediction: Experiments with an intermediate coupled model. *Journal of Climate*, *17*, 3057–3073.

Mu, M., Duan, W. S., Chen, D., & Yu, W. D. (2015). **Target observations for improving initialization of high-impact ocean-atmospheric environmental events forecasting**. *National Science Review*, *2*, 226–236.

Mu, M., Duan, W.S., & Chou, J. F. (2004). Recent advances in predictability studies in China (1999–2002). *Advances in Atmospheric Sciences*, *21*, 437–443.

Mu, M., Duan, W. S., & Wang, B. (2003). Conditional nonlinear optimal perturbation and its applications. *Nonlinear Processes in Geophysics*, *10*, 493–501.

Mu, M., Duan, W. S., & Wang, B. (2007a). Season-dependent dynamics of nonlinear optimal error growth and El Niño-Southern Oscillation predictability in a theoretical model. *Journal of Geophysical Research*, *112*, D10113.

Mu, M., Duan, W. S., & Wang, J. C. (2002). The predictability problems in numerical weather and climate prediction. *Advances in Atmospheric Sciences*, *19*, 191–204.

Mu, M., Duan, W. S., Wang, Q., & Zhang, R. (2010). An extension of conditional nonlinear optimal perturbation approach and its applications. *Nonlinear Processes in Geophysics*, *17*, 211–220.

Mu, M., & Ren, H. L. (2017). Enlightenments from researches and predictions of 2014–2016 super El Niño event. *Science China: Earth Sciences*, *60*, 1569–1571.

Mu, M., Xu, H., & Duan, W. S. (2007b). A kind of initial perturbations related to "spring predictability barrier" for El Niño events in Zebiak-Cane model. *Geophysical Research Letters*, *34*, L03709.

Mu, M., Yu, Y. S., Xu, H., & Gong, T. T. (2014). Similarities between optimal precursors for ENSO events and optimally growing initial errors in El Niño predictions. *Theoretical and Applied Climatology*, *115*, 461–469.

Mu, M., & Zhang, Z. (2006). Conditional nonlinear optimal perturbations of a two-dimensional quasigeostrophic model. *Journal of Atmospheric Sciences*, *63*, 1587–1604.

Palmer T. N., Andersen, U., Cantelaube, P., Alessandri A., Gualdi, S., Andersen U., . . . Thomson, M. C. (2004). Development of a European multimodel ensemble system for seasonal to interannual prediction (DEMETER). *Bulletin of the American Meteorological Society*, *85*, 853–872.

Palmer, T. N., Branković, Č., Viterbo, P., & Miller, M. J. (1992). Modeling interannual variations of summer monsoons. *Journal of Climate*, *5*, 399–417.

Palmer, T. N., Buizza, R., Molteni, F., & Corti, S. (1994). Singular vectors and the predictability of weather and climate. *Philosophical Transactions Physical Sciences & Engineering*, *348*, 459–475.

Palmer, T. N., Gelaro, R., Barkmeijer, J., & Buizza, R. (1998). Singular vectors metrics and adaptive observations. *Journal of Atmospheric Sciences*, *55*, 633–653.

Palmer, T. N., & Zanna, L. (2013). Singular vectors, predictability and ensemble forecasting for weather and climate. *Journal of Physics A: Mathematical and Theoretical*, *46*(25), 254018.

Philander, S. G. H. (1983). El Niño Southern Oscillation phenomena. *Nature*, *302*, 295–301.

Qi, Q. Q., Duan, W. S., Zheng, F., & Tang, Y. M. (2016). **Using an ICM ensemble prediction system outputs to explore the "spring predictability barrier" for 2015/2016 El Niño event**. *Science China Earth Sciences*, *60*, 1614 Chin.

Rasmusson, E. M., & Carpenter, T. H. (1982). Variations in tropical sea surface temperature and surface wind fields associated with the Southern Oscillation/El Niño. *Monthly Weather Review*, *110*, 354–384.

Rasmusson, E. M, & Wallace, J. M. (1983). Meteorological aspects of the El Niño/Southern Oscillation. *Science*, *222*, 1195–1202.

Roads, J. O. (1987). Predictability in the extended range. *Journal Atmospheric Sciences*, *44*, 1228–1251.

Ropelewski, C. F., & Halpert, M. S. (1987). Global and regional scale precipitation patterns associated with the El Niño Southern Oscillation. *Monthly Weather Review*, *115*, 1606–1626.

Saha, S., Nadiga, S., Thiaw, C., Wang, J., Wang, W., Zhang, Q., . . . Xie, P. (2006). The NCEP climate forecast system. *Journal of Climate*, *19*, 3483–3517.

Saji, N. H., & Yamagata, T. (2003). Possible impacts of Indian Ocean dipole mode events on global climate. *Climate Research*, *25*(2), 151–169.

Samelson, R. M., & Tziperman, E. (2001). Instability of the chaotic ENSO: The growth-phase predictability barrier. *Journal of Atmospheric Sciences*, *58*, 3613–3625.

Smith, L. A., Ziehmann, C., & Fraedrich, K. (1999). Uncertainty dynamics and predictability in chaotic systems. *Quarterly Journal of the Royal Meteorological Society*, *125*, 2855–2886.

Snyder, C. (1996). Summary of an informal workshop on adaptive observations and FASTEX. *Bulletin of the American Meteorological Society*, *77*, 953–961.

Stein, K., Schneider, N., Timmermann, A., & Jin, F. F. (2010). Seasonal synchronization of ENSO events in a linear stochastic model. *Journal of Climate*, *23*, 5629–5643.

Stein, K., Timmermann, A., Schneider N., Jin, F. F., & Stuecker, M. F. (2014). ENSO seasonal synchronization theory. *Journal of Climate*, *27*, 5285–5310.

Syu, H. H., & Neelin, J. D. (2000). ENSO in a hybrid coupled model. Part I: sensitivity to physical parametrizations. *Climate Dynamics*, *16*(1), 19–34.

Takahashi, K., Montecinos, A., Goubanova, K., & Dewitte, B. (2011). Enso regimes: Reinterpreting the canonical and Modoki El Niño. *Geophysical Research Letters*, *38*, L10707.

Tang, Y. M., Kleeman, R., & Moore, A. M. (2008). Comparison of information-based measures of forecast uncertainty in ensemble ENSO prediction. *Journal of Climate*, *21*, 230–247.

Tang, Y. M., Kleeman, R., Moore, A. M., Weaver, A., & Vialard, J. (2003). **The use of ocean reanalysis products to initialize ENSO predictions**. *Geophysical Research Letters*, *30*, 1694.

Tennekes, H. (1991). Karl Popper and the accountability of numerical forecasting. In *New developments in Predictability: Proceedings of a workshop held at ECMWF 13–15 November 1991*. Reading, UK: European Centre for Medium-Range Weather Forecasts. Conference paper.

Thompson, C. J. (1998). *A linear, stochastic, dynamical model of El Niño–Southern Oscillation* (Doctoral dissertation abstract). University of Washington. Retrieved from Abstracts International, 59–03 (Section B), p. 1161.

Thompson, C. J., & Battisti, D. S. (2001). A linear stochastic dynamical model of ENSO. Part II: Analysis. *Journal of Climate*, *14*, 445–466.

Thompson, P. D. (1957). Uncertainty of initial state as a factor in the predictability of large scale atmospheric flow patterns. *Tellus*, *9*, 275–295.

Tian, B., & Duan, W. S. (2016). **Comparison of the initial errors most likely to cause a spring predictability barrier for two types of El Niño events**. *Climate Dynamics*, *47*, 779–792.

Torn, R. D. (2016). Evaluation of atmosphere and ocean initial condition uncertainty and stochastic exchange coefficients on ensemble tropical cyclone intensity forecasts. *Monthly Weather Review*, *144*, 3487–3506.

Toth, Z., & Kalnay, E. (1996). Ensemble forecasting at NCEP. Seminar Proceedings of a Workshop on Predictability, Volume 2, ECMWF, Shinfield Park, Reading, UK, pp. 39–60.

Trenberth, K. E., Branstator, G. W., Karoly, D., Kumar, A., Lau, N. C., & Ropelewski, C. (1998). **Progress during TOGA in understanding and modeling global**

teleconnections associated with tropical sea surface temperatures. *Journal of Geophysical Research: Oceans*, *103*, 14291–14324.

Tziperman, E., & Ioannou, P. J. (2002). Transient growth and optimal excitation of thermohaline variability. *Journal of Physical Oceanography*, *32*, 3427–3435.

U.S. CLIVAR Project Office. (2013). *2012 U.S. CLIVAR Summit Report* (Report 2013–4). U.S. CLIVAR Project Office, Washington, DC.

van Oldenborgh, G. J., Burgers, G., Venzke, S., Eckert, C., & Giering, R. (1999). Tracking down the ENSO delayed oscillator with an adjoint OGCM. *Monthly Weather Review*, *127*, 1477–1496.

van Oldenborgh, G. J., Philip, S. Y., & Collins, M. (2005). El Niño in a changing climate: A multi-model study. *Ocean Science*, *1*, 81–95.

Wang, B., & Fang, Z. (1996). Chaotic oscillation of tropical climate: A dynamic system theory for ENSO, J *Atmospheric Sciences*, *53*, 2786–2802.

Wang, C. Z., & Picaut, J. (2004). Understanding ENSO physics: A review. In C. Wang, S. P. Xie, & J. A. Carton (Eds.), *Earth climate: The ocean-atmosphere interaction* (pp. 21–48). Geophysical Monograph Series 147. Washington, DC: American Geophysical Union.

Webster, P. J., & Yang, S. (1992). Monsoon and ENSO: Selectively interactive systems. *Quarterly Journal of the Royal Meteorological Society*, *118*, 877–926.

Weng, H. Y., Ashok, K., Behera, S. K., Rao, S. A., & Yamagata, T. (2007). Impacts of recent El Niño Modoki on dry/wet conditions in the Pacific rim during boreal summer. *Climate Dynamics*, *29*, 113–129.

Williams, P. D. (2005). Modeling climate change: The role of unresolved processes. *Philosophical Transactions of the Royal Society A: Mathematical. Physical and Engineering Sciences*, *363*, 2931–2946.

Wu, C. C., Chen, J. H., Lin, P. H., & Chou, K. H. (2007). Targeted observations of tropical cyclone movement based on the adjoint-derived sensitivity steering vector. *Journal of Atmospheric Sciences*, *64*, 2611–2626.

Wu, B., & Zhou, T. J. (2012). Prediction of decadal variability of sea surface temperature by a coupled global climate model FGOALS_gl developed in LASG/IAP. *Chinese Science Bulletin*, *57*, 2453–2459.

Wu, D. H., Anderson, D. L. T., & Davey, M. K. (1993). ENSO variability and external impacts. *Journal of Climate*, *6*, 1703–1717.

Xue, Y., Cane, M. A., & Zebiak, S. E. (1997a). Predictability of a coupled model of ENSO using singular vector analysis. Part I: optimal growth in seasonal background and ENSO cycles. *Monthly Weather Review*, *125*, 2043–2056.

Xue, Y., Cane, M. A., & Zebiak, S. E. (1997b). Predictability of a coupled model of ENSO using singular vector analysis. Part II: Optimal growth and forecast skill. *Monthly Weather Review*, *125*, 2057–2073.

Xue, Y., Cane, M. A., Zebiak, S. E., & Blumenthal, M. B. (1994). On the prediction of ENSO: A study with a low-order Markov model. *Tellus A*, *46*, 512–528.

Yamaguchi M., Iriguchi T., Nakazawa, T., & Wu, C. C. (2009). An observing system experiment for Typhoon Conson (2004) using a singular vector method and DOTSTAR data. *Monthly Weather Review*, *137*, 2801–2816.

Yeh, S. W., Ham, Y. G., & Lee, J. Y. (2012). Changes in the Tropical Pacific SST Trend from CMIP3 to CMIP5 and its implication of ENSO. *Journal of Climate*, *25*, 7764–7771.

Yu, J. Y., & Kim, S. T. (2010). **Identification of central-Pacific and eastern-Pacific types of ENSO in CMIP3 models**. *Geophysical Research Letters*, *137*, L15705.

Yu, J. Y., & Kim, S. T. (2011). Relationships between extratropical sea level pressure variations and the central Pacific and eastern Pacific types of ENSO. *Journal of Climate*, *24*, 708–720.

Yu, L. S., Weller, R. A., & Liu, T. W. (2003). **Case analysis of a role of ENSO in regulating the generation of westerly wind bursts in the Western Equatorial Pacific**. *Journal of Geophysical Research-Oceans*, *108*, 3128.

Yu, L., Mu, M., & Yu, Y. S. 2014. Role of parameter errors in the spring predictability barrier for ENSO events in the Zebiak-Cane model. *Advances in Atmospheric Sciences*, *31*, 647–656.

Yu, Y. S., Duan, W. S., Xu, H., & Mu, M. (2009). Dynamics of nonlinear error growth and season-dependent predictability of El Niño events in the Zebiak-Cane model. *Quarterly Journal of the Royal Meteorological Society*, *135*, 2146–2160.

Yu, Y. S., Mu, M., & Duan, W. S. (2012). Does model parameter error cause a significant “spring predictability barrier” for El Niño events in the Zebiak-Cane model? *Journal of Climate*, *25*, 1263–1277.

Yu, Y. S., Mu, M., Duan, W. S., & Gong, T. T. (2012). Contribution of the location and spatial pattern of initial error to uncertainties in El Niño predictions. *Journal of Geophysical Research*, *117*, 1–13.

Yuan, D., Zhou, H., & Zhao, X. (2013). Interannual climate variability over the tropical Pacific Ocean induced by the Indian Ocean dipole through the Indonesian throughflow. *Journal of Climate*, *26*, 2845–2861.

Zanna, L. (2012). Forecast skill and predictability of observed Atlantic sea surface temperatures. *Journal of Climate*, *25*, 5047–5056.

Zavala-Garay, J., Moore, A. M., & Kleeman, R. (2004). Influence of stochastic forcing on ENSO prediction. *Journal of Geophysical Research: Oceans*, *109*, C11007.

Zebiak, S. E. (1989). On the 30–60 day oscillation and the prediction of El Niño. *Journal of Climate*, *15*, 1381–1387.

Zebiak, S. E., & Cane, M. A. (1987). A model El Niño Southern Oscillation. *Monthly Weather Review*, *115*, 2262–2278.

Zhang, H. H., Clement, A., & Di Nezio, P. (2014). The South Pacific meridional mode: A mechanism for ENSO-like variability. *Journal of Climate*, *27*, 769–783.

Zhang, J., Duan, W. S., & Zhi, X. F. (2015). Using CMIP5 model outputs to investigate the initial errors that cause the “spring predictability barrier” for El Niño events. *Science China Earth Sciences*, *58*(5), 1–12.

Zhang, R. H., Zebiak, S. E., Kleeman, R., & Keenlyside, N. (2003). **A new intermediate coupled model for El Niño simulation and prediction**. *Geophysical Research Letters*, *30*, 153–166.

Zhou, Q., Duan, W. S., Mu, M., & Feng, R. (2015). Influence of positive/negative Indian Ocean dipole on Pacific ENSO through Indonesian throughflow: Results from sensitivity experiments. *Advances in Atmospheric Sciences*, *32*, 783–793.

Mu Mu

Chinese Academy of Sciences